
Article:
Pickup, B.T. orcid.org/0000-0002-2728-5486 and Fowler, P.W. orcid.org/0000-0003-2106-1104 (2020) A correlated source-sink-potential model consistent with the Meir–Wingreen formula. The Journal of Physical Chemistry A, 124 (34). pp. 6928-6944. ISSN 1089-5639

https://doi.org/10.1021/acs.jpca.0c01711

A Correlated Source-Sink-Potential Model Consistent with the Meir-Wingreen Formula

Barry T. Pickup* and Patrick W. Fowler*

Department of Chemistry, University of Sheffield, Sheffield, S3 7HF, UK

E-mail: B.T.Pickup@sheffield.ac.uk; P.W.Fowler@sheffield.ac.uk

Abstract

We model a molecular device as a molecule attached to a set of leads treated at the tight-binding level, with the central molecule described to any desired level of electronic structure theory. Within this model, in the absence of electron-phonon interactions, the Landauer-Büttiker part of the Meir-Wingreen formula is shown to be sufficient to describe the transmission factor of the correlated device. The key to this demonstration is to ensure that the correlation self-energy has the same functional form as the exact correlation self-energy. This form implies that non-symmetric contributions to the Meir-Wingreen formula vanish, and hence conservation of current is achieved without the need for Green's Function self-consistency. An extension of the Source-Sink-Potential (SSP) approach gives a computational route to the calculation and interpretation of electron transmission in correlated systems. In this picture, current passes through internal molecular channels via resonance states with complex-valued energies. Each resonant state arises from one of the states in the Lehmann expansion of the one-electron Green's Function, hole conduction deriving from ionised states, and particle conduction from attached states. In the correlated device, the dependence of transmission on electron energy is determined by four structural polynomials, as it was in the tight-binding (Hückel) version of the SSP method. Hence, there are active and inert conduction channels (in the correlated case, linked to Dyson orbitals) governed by a set of selection rules that map smoothly onto the simpler picture.

1 Introduction

The possibility of constructing devices from single molecules was modelled by Aviram and Ratner as long ago as 1974.[1] The intervening half century has seen the growth of a vast research literature on nanoscale devices, comprising thousands of theoretical and experimental papers, reviews and books.[2–8] There are many interesting phenomena observed in connection with nanoscale devices, such as Coulomb blockade, the Kondo effect, negative differential resistance, current rectification, current bistability and hysteresis. These non-linear effects are described in the reviews listed above. The simplest nanoscale molecular electronic device (MED) is generally recognised as being composed of three parts (see Fig. 1a), a left lead (L) attached to a molecule (M), the latter being attached to a right lead (R). The lead L may be regarded as a source of electrons, whilst the lead R is a sink. Landauer[9] wrote the conductance for an electron of given spin σ passing through a single-channel lead as

$$\mathcal{G}_\sigma = \mathcal{G}_0 T_\sigma, \tag{1}$$

where T_σ is the probability of transmission for elastic scattering of electrons of fixed spin σ. The quantity

$$\mathcal{G}_0 = \frac{e^2}{h} \approx (25.8\ \mathrm{k\Omega})^{-1}, \tag{2}$$

is interpreted as the 'quantum of conductance' between leads and molecule.[10] Conversely, h/e^2 is the quantum unit of resistance for the transmission through a nanoscale device. It implies,

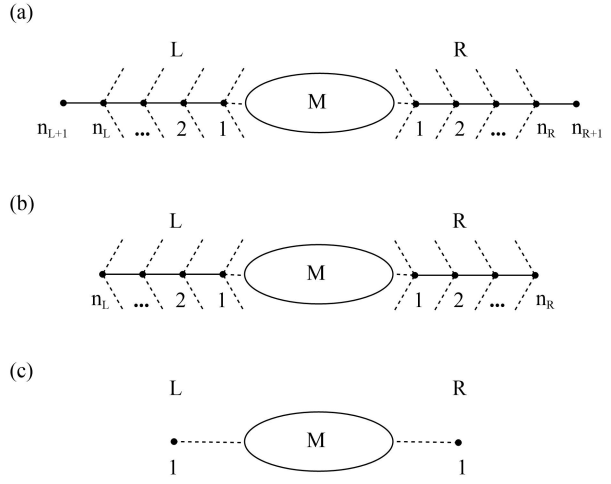

Figure 1: a) A molecule, M, attached to semi-infinite left- and right-hand wires, L and R, showing the numbering scheme adopted for atoms in the wires. b) The SSP molecular device, comprising a molecule attached to source and sink atoms $n_{\rm L}$ and $n_{\rm R}$ via multiple contacts in the molecule. Dotted lines indicate molecule-lead contact interactions. c) SSP model of the two-lead device with *simple* connections, where $n_{\rm L} = n_{\rm R} = 1$, and each lead terminal atom is connected to exactly one atom in the molecule.

for a bias voltage of 1 V, that approximately 5×10^{14} electrons (of both spins) pass through the device, with a transit time of around 2 fs.[11] This time is short compared to a typical molecular bond vibration with a frequency of around 10^{-14} Hz, which suggests that transmission is a purely electronic process with no vibronic component. The regime in which electrons are transported through the molecule without exchange of energy, i.e. with elastic scattering, is known as the coherent tunnelling regime. It dominates the transport process when the electron residence time in the MED is short compared to the time needed to excite electronic or vibronic excitations. However, measured resistances in many cases are greater by orders of magnitude than the 25.8 kΩ quoted above. In such situations vibronic (phonon) inelastic scattering interactions become important (see Ref. 12 chapter 16). In cases where the lead-molecule interaction is weak, and when temperatures are low, the electron-electron interaction dominates, and one enters the Coulomb blockade regime. This manifests itself in terms of a series of steps in the device I-V curve. These steps are produced by changes in the number of electrons occurring when the applied bias is large enough.

Scattering approaches to MEDs have been developed using a Green's function (GF) formalism by Ratner et al.[13–15] and Datta et al.[16,17] The Landauer-Büttiker (LB) formula for the transmission of an electron with spin σ, in a.u. for a device with a single eigenmode is[13]

$$T_\sigma = {\rm tr}\mathbf{G}^{\rm r}_{\rm MM}\mathbf{\Gamma}^{\rm L}_{\rm MM}\mathbf{G}^{\rm a}_{\rm MM}\mathbf{\Gamma}^{\rm R}_{\rm MM}, \qquad (3)$$

where the matrices $\mathbf{\Gamma}^{\rm L}_{\rm MM}$ and $\mathbf{\Gamma}^{\rm R}_{\rm MM}$ are the scattering (also known as tunnelling) rate matrices for leads L and R. The quantities $\mathbf{G}^{\rm r,a}_{\rm MM}$ are the retarded and advanced *molecular* GFs (c.f. section 2.3) defined in the presence of interaction with the leads. The total current, allowing for the distribution of electrons in the leads is,[12]

$$J_\sigma = \frac{1}{2\pi}\int T_\sigma(f_{\rm L} - f_{\rm R})dE, \qquad (4)$$

where the Fermi distribution function, $f_{\rm X}$ for X = L or R, is

$$f_{\rm X} = [\exp((E-\mu_{\rm X})/k_{\rm B}T) + 1]^{-1}, \qquad (5)$$

and $\mu_{\rm X}$ is the chemical potential in lead X. The flow of particles and holes through the device in Eq. (4) is determined by the balance of chemical potentials in the two leads, and the transmission, $T_\sigma(E)$.

The LB formula was derived assuming that the electrons in the device were non-interacting. Interaction effects have been included in theories of transmission in the work of Caroli et. al.,[18] and Meir and Wingreen.[19] Meir and Wingreen recognised that the MED is not in equilibrium, and hence used the non-equilibrium GF (NEGF) method[20–23] to derive equations for the current through a *steady-state* molecular device. The Meir-Wingreen (MW) formula for the current of spin σ elec-

trons through lead L is

$$J_{\mathrm{L}\sigma} = i \int \frac{dE}{2\pi} \mathrm{tr} \mathbf{\Gamma}^{\mathrm{L}}_{\mathrm{MM}} (f_{\mathrm{L}} \Delta \mathbf{G}_{\mathrm{MM}} + \mathbf{G}^{<}_{\mathrm{MM}}), \quad (6)$$

In Eq. (6) we adopt a convenient notation

$$\Delta \mathrm{X} = \mathrm{X}^{\mathrm{r}} - \mathrm{X}^{\mathrm{a}}, \quad (7)$$

which we will use throughout this paper for the difference between retarded and advanced forms of various quantities. The retarded, advanced and lesser molecular GFs (see section 2.3) include effects of lead-molecule and electron-electron interactions. Eq. (6) is clearly not symmetric in terms of the lead indices, L and R, but a symmetrized version[19] is often used in computations.

The most popular computational methods based on the MW formula use density functional theory (DFT) to describe electron-electron interactions.[24–26] These methods assume that the (retarded and advanced) GFs can be expanded in Lehmann[27] form in terms of the Kohn-Sham (KS) orbitals and orbital energies. This implies that the KS orbital energies are sufficiently accurate representations of the ionisation and attachment energies of the molecule. It is true that the HOMO orbital energy is, in the limit of the *exact* DFT functional, equal to the *exact* ionisation energy, but the situation for other energy levels, and especially the attachment spectrum, is uncertain.[28,29] Furthermore, standard DFT functionals underestimate the fundamental (HOMO-LUMO) molecular gap.[30–34] The true form of the complete GF as a functional of the electron density is unknown, although a 'complex orbital' DFT for non-equilibrium systems has been derived.[35] In practice, calculations use various standard (i.e. relevant to equilibrium ground states) approximate exchange-correlation potentials, and that predicted transmission can vary by an order of magnitude depending on this choice.[36] Notwithstanding these problems, DFT has been very successful in predicting transmission in strongly coupled systems in the coherent tunnelling regime. Transmission in weakly coupled systems, on the other hand, tends to be overestimated.[37]

It has been traditional in theoretical physics to use the 'equations of motion' (EOM) technique to calculate GFs. The EOM are generated from the commutation relations between creation operators and the Hamiltonian. They give chains of matrix relations that are often truncated in an ad hoc manner. This technique has been applied with success to coupled quantum dots.[38–41]

An alternative approach is to use a correlated GF based upon the GW method,[42] which expresses the self-energy as $G \times W$, where G is the GF, and W is the screened electron-electron interaction arising from the sea of electrons. Since the self-energy is itself used to determine G, the GW method requires iteration to self-consistency. Whilst this is computationally expensive, it has the advantage that the resulting GF can be shown to satisfy conservation rules in terms of the electronic charge,[27] and hence the computed transmissions through leads L and R are necessarily equal. A number of GW calculations of MED conduction have appeared.[37,43,44] A comparison of DFT and GW approaches has been published by Solomon et al.[45]

The methods discussed thus far are very effective in dealing with the coherent tunnelling regime where there are fixed numbers of electrons on the molecule. The Master Equation approach is more appropriate for treating the Coulomb blockade regime.[46–49] Sophisticated methods for dealing with both coherent tunnelling and Coulomb blockade have recently been developed.[50]

Our approach in the current paper is to link the sophisticated theoretical approaches outlined above with the simpler Source-Sink-Potential (SSP) model proposed by Ernzerhof and co-workers.[51,52] This model has significant advantages for interpretation and design. From the SSP model in its graph-theoretical formulation[53] it is possible to derive clear links between molecular electronic structure of a π system and predicted transmission for a given device connection pattern. The graph-theoretical approach has also been used to link conductivity to chemical concepts such as 'curly arrow' mnemonics.[54,55] It is also possible to use SSP directly in ab initio calculations.[56]

In the present work we consider the steady state of an SSP-like model with one-electron leads, a one-electron contact interaction and a molecule with two-electron interactions. Under these assumptions the MW formula, Eq (6), separates formally into *Landauer*and *non-Landauer* contributions. We show that the Landauer part is equivalent to the LB formula in Eq (3), but containing correlated molecular GFs. We also show that the non-Landauer contribution is *exactly zero* for a self-energy having the functional form of the exact correlation self-energy. We then derive an extended version of the SSP formalism that is equivalent to this correlated Landauer-Büttiker formula. This allows a seamless progression in level of treatment and interpretation of the molecular component of a device, from tight-binding, through self-consistent-field theory to correlated Hamiltonians.

For design of MEDs, an intuitive understanding of the nature of the internal channels for conduction through a molecule is advantageous. It has been noted in the literature[57] that these internal channels are poorly understood, but their connection with molecular orbital symmetry has been noted by Solomon.[58] A link between sophisticated and model calculations, as an aid to interpretation, has also been provided by Borges.[59] Quantum interference effects are often characterised by reversals and bifurcations of ring current.[60–63] As a cautionary note, Solomon et al.[64] have also shown that through-space, rather than through-bond, terms frequently dominate conduction through a molecular bridge.

A simplified graphical method has been described[65] for prediction of antiresonances, i.e. of vanishing transmission. Ernzerhof[66] has used simple chemical ideas and his SSP model to provide understanding of ballistic transmission in nanographenes. The SSP model has also been used successfully[53,67–75] to interpret molecular conduction in terms of the internal conduction channels provided by Hückel molecular orbitals. These channels can be active or inert,[73] and the transmission spectrum follows interpreted in terms of selection rules.[76] The emphasis of the present paper is to show that these advantages are retained in a more realistic correlated description of the central molecule.

Ernzerhof[77] has formulated a correlated SSP method based on a CI wavefunction for a device with a fixed number of molecular electrons and a single scattered electron. This gives a natural description of Pauli Blockade,[12] but does not allow for the possibility of hole conduction. A similar restriction applies to our own versions of the CI-based SSP method.[74] Such methods are appropriate for devices composed of quantum dots, where Pauli blockade has been observed experimentally.[78,79] In contrast, the GF-based correlated SSP method proposed here is even-handed in its treatment of particle and hole conduction.

The structure of the paper is as follows. Section 2 presents the required theory and is divided into subsections. We reprise the SSP model of molecular transmission (2.1), describe the device Hamiltonian (2.2), give a brief introduction to Green's functions (2.3), and the MW formula (2.4), and the roles of Landauer and non-Landauer contributions. The theory section continues with the explicit connection between the NEGF and SSP methods (2.5), shows how an extended correlated SSP model can be built, and describes how the concepts of the tight-binding SSP model are preserved in the extended model (2.6). Specimen calculations are presented in Section 3. Section 4 gives a discussion of our main findings, and Section 5 draws general conclusions.

2 Theory

2.1 SSP Transmission

To begin with, we restrict our discussion to a Hückel (tight-binding) model. We assume that the molecule has a single resonance parameter β_{M}, and coulomb parameter α_{M}. In the usual system of units, α_{M} is set to zero, and β_{M} is taken as -1 so that α_{M} acts as the origin, and $|\beta_{\mathrm{M}}|$ as a natural unit for energy level diagrams. The molecular adjacency matrix, $\mathbf{A}$, has $A_{\mathrm{pq}} = \beta_{\mathrm{M}}$ if $\mathrm{p} \neq \mathrm{q}$ and p is bonded to q, (p$\sim$q,) and $A_{\mathrm{pq}} = 0$ otherwise. We consider a

connection in which single molecular atoms $\overline{\mathrm{L}}$ and $\overline{\mathrm{R}}$ interact with the terminal atoms L and R of the leads via connection matrix elements $\beta_{\overline{\mathrm{L}}\,\mathrm{L}}$ and $\beta_{\overline{\mathrm{R}}\,\mathrm{R}}$, respectively. We shall refer to this as a *simple* connection between molecule and leads (see Fig. 1c), compared to the *general* connection shown in Fig. 1b, which has multiple lead-molecule interactions and will be treated in section 2.5.

We have previously derived analytical expressions for electronic transmission in a device with simple single-atom connections.[53,67–72,76] For an incoming beam of electrons with energy E, these solutions are written in terms of five molecular *structural* polynomials (SP), which comprise graph-theoretical characteristic polynomials[53]

$$\begin{aligned} s &= \det\left(E\mathbf{1}-\mathbf{A}\right), \\ t &= \det\left(E\mathbf{1}-\mathbf{A}\right)^{\left[\overline{\mathrm{L}},\overline{\mathrm{L}}\right]}, \\ u &= \det\left(E\mathbf{1}-\mathbf{A}\right)^{\left[\overline{\mathrm{R}},\overline{\mathrm{R}}\right]}, \\ v &= \det\left(E\mathbf{1}-\mathbf{A}\right)^{\left[\overline{\mathrm{L}}\,\overline{\mathrm{R}},\overline{\mathrm{L}}\,\overline{\mathrm{R}}\right]}, \\ \jmath &= (-1)^{\overline{\mathrm{L}}+\overline{\mathrm{R}}}\det\left(E\mathbf{1}-\mathbf{A}\right)^{\left[\overline{\mathrm{L}},\overline{\mathrm{R}}\right]}, \end{aligned} \tag{8}$$

where the superscripts in braces indicate the rows (left) and columns (right) corresponding to connection atoms $\overline{\mathrm{L}}$ and $\overline{\mathrm{R}}$ that are to be struck out from the characteristic matrices. Only four of the polynomials are independent. The polynomial, $\jmath$, with row $\overline{\mathrm{L}}$ and column $\overline{\mathrm{R}}$ removed from the determinant, satisfies the Jacobi-Sylvester relation[80]

$$\jmath^2 = ut - sv. \tag{9}$$

The expression for the overall transmission of SSP devices is then[53]

$$T\left(E\right) = \mathcal{B}\frac{j^2}{|D|^2}, \tag{10}$$

where

$$\mathcal{B} = 4\beta_{\mathrm{L}}\beta_{\mathrm{R}}\sin q_{\mathrm{L}}\sin q_{\mathrm{R}}(\beta_{\overline{\mathrm{L}}\,\mathrm{L}}\beta_{\overline{\mathrm{R}}\,\mathrm{R}})^2. \tag{11}$$

The function in the denominator is

$$\begin{aligned} D(E) = {} & \beta_{\mathrm{L}}e^{-iq_{\mathrm{L}}}\beta_{\mathrm{R}}e^{-iq_{\mathrm{R}}}s - \beta_{\mathrm{R}}e^{-iq_{\mathrm{R}}}\beta_{\overline{\mathrm{L}}\,\mathrm{L}}^2 t \\ & - \beta_{\mathrm{L}}e^{-iq_{\mathrm{L}}}\beta_{\overline{\mathrm{R}}\,\mathrm{R}}^2 u + \beta_{\overline{\mathrm{L}}\,\mathrm{L}}^2\beta_{\overline{\mathrm{R}}\,\mathrm{R}}^2 v. \end{aligned} \tag{12}$$

The wavevectors q_{L} and q_{R} are functions of E satisfying the dispersion relations

$$E = \alpha_{\mathrm{L}} + 2\beta_{\mathrm{L}}\cos q_{\mathrm{L}} = \alpha_{\mathrm{R}} + 2\beta_{\mathrm{R}}\cos q_{\mathrm{R}}, \tag{13}$$

appropriate for the semi-infinite wires in Fig. 1b, assuming Hückel parameters $(\alpha_{\mathrm{L}}, \beta_{\mathrm{L}})$ and $(\alpha_{\mathrm{R}}, \beta_{\mathrm{R}})$ within left and right wires, respectively.

It is convenient to define reduced 'hatted' SPs as the ratios

$$\hat{t} = t/s,\ \hat{u} = u/s,\ \hat{\jmath} = \jmath/s,\ \hat{v} = v/s. \tag{14}$$

The hatted SPs, together with the definition $\hat{D} = D/s$, give Eq. (10) in scaled form as

$$T\left(E\right) = \mathcal{B}\frac{\hat{\jmath}^2}{|\hat{D}|^2}. \tag{15}$$

The SPs s, t, u, and v are characteristic polynomials of the molecular graph G, and the three vertex-deleted subgraphs $G-\overline{\mathrm{L}}$, $G-\overline{\mathrm{R}}$ and $G-\overline{\mathrm{L}}-\overline{\mathrm{R}}$. The formulas (10) and (15) show the direct link between transmission and the pattern of connections for this simplest possible model of the molecular electronic structure.

The hatted SPs also provide a first contact between SSP and GF methods, since they are equal to matrix elements of the GF in the AO basis for the one-electron Hückel Hamiltonian:

$$\mathbf{g}_{\mathrm{MM}}^{\mathrm{H\ddot{u}ck}} = (E\mathbf{1}-\mathbf{A})^{-1}. \tag{16}$$

We can write them as spectral resolutions,

$$\begin{aligned} \hat{t} &= \sum_{\lambda}\frac{|U_{\overline{\mathrm{L}}\,\lambda}|^2}{E-\epsilon_\lambda} &&= \mathbf{g}_{\mathrm{MM}}^{\mathrm{H\ddot{u}ck}}(E)_{\overline{\mathrm{L}}\,\overline{\mathrm{L}}}, \\ \hat{u} &= \sum_{\lambda}\frac{|U_{\overline{\mathrm{R}}\,\lambda}|^2}{E-\epsilon_\lambda} &&= \mathbf{g}_{\mathrm{MM}}^{\mathrm{H\ddot{u}ck}}(E)_{\overline{\mathrm{R}}\,\overline{\mathrm{R}}}, \\ \hat{\jmath} &= \sum_{\lambda}\frac{U_{\overline{\mathrm{L}}\,\lambda}U_{\overline{\mathrm{R}}\,\lambda}^*}{E-\epsilon_\lambda} &&= \mathbf{g}_{\mathrm{MM}}^{\mathrm{H\ddot{u}ck}}(E)_{\overline{\mathrm{L}}\,\overline{\mathrm{R}}}, \end{aligned} \tag{17}$$

in which the ϵ_λ are Hückel MO energies, and

the $U_{p\lambda}$ are expansion coefficients for the corresponding eigenvectors. The polynomial $\hat{v}$ is also related to the Hückel GF matrix elements through Eq. (9).

This method may seem limited theoretically in that it is based on a tight-binding (Hückel theory) description of electronic structure. However, it has enabled us to recognise that conduction in a specific device can be understood in terms of internal molecular channels associated with the molecular orbitals, that these channels produce the peaks in the transmission spectrum, and can be classified according to a small set of *conduction cases*[76] depending upon the multiplicities of the roots of the structural polynomials (SPs) defined in Eq. (8). Furthermore, internal channels can be classified as *inert* or *active*.[73] The advantages to be gained by interpreting the conduction process in this way are significant.

2.2 The Device Hamiltonian

A note on the underlying device Hamiltonian is required, as we intend to consider a more general molecular Hamiltonian. The device comprises two leads, left (L), right (R), and a molecule (M), with device Hamiltonian

$$H = H_{\rm M} + H_{\rm L} + H_{\rm R} + V, \qquad (18)$$

where the perturbation, V, contains the interaction terms between the molecule and leads. The perturbation is switched on adiabatically at time $t = -\infty$, so that at finite times the system has evolved into a fully interacting device that can be considered to be in a steady state. There is no flow of current in the unperturbed system, since it comprises separate leads and molecule, each of which is in an equilibrium state.

Our focus will be on conduction through a correlated molecule, so we adopt a molecular Hamiltonian that contains two-electron interactions,viz.

$$H_{\rm M} = \sum_{\rm pq} h_{\rm pq} a_{\rm p}^\dagger a_{\rm q} + \frac{1}{2}\sum_{\rm pqrs} \langle {\rm pr}|{\rm qs}\rangle a_{\rm p}^\dagger a_{\rm r}^\dagger a_{\rm q} a_{\rm s}, \qquad (19)$$

where we have expressed the Hamiltonian in terms of a basis of orthonormal spin-orbitals. This is, in principle, the exact non-relativistic (spinless) Born-Oppenheimer Hamiltonian. However, in practice any set of orthonormal spin-orbitals, $\{\psi_{\rm p}\}$, will be finite and hence incomplete.

One might choose a model Hamiltonian representation in which molecular one- and two-electron integrals ($h_{\rm pq}$ and $\langle {\rm pr}|{\rm qs}\rangle$) were either parameterised or computed ab initio. In the former case, there is a range of possibilities, from the strictly one-electron Hückel model, through Hubbard[81] or PPP.[82–84] In the latter, DFT or ab initio models could be used.

The Hamiltonian for each lead is that for a Hückel (tight-binding) semi-infinite chain,

$$H_{\rm X} = \alpha_{\rm X}\sum_{\rm p} a_{\rm p}^\dagger a_{\rm p} + \beta_{\rm X}\sum_{\rm p\sim q} a_{\rm p}^\dagger a_{\rm q}, \qquad (20)$$

with X = L, or R, and p∼q restricting the summation to directly bonded atoms. Coulomb and resonance parameters, $(\alpha_{\rm X}, \beta_{\rm X})$, completely specify the leads, and each lead is a source or sink of electrons (or holes) conducted through the molecule.

The Hamiltonian for connection between molecule and leads, V, is written as

$$V = V_{\rm LM} + V_{\rm RM} + V_{\rm ML} + V_{\rm MR}, \qquad (21)$$

where

$$V_{\rm XM} = \sum_{\rm p\in X, q\in M} h_{\rm pq} a_{\rm p}^\dagger a_{\rm q}, \qquad (22)$$

and $V_{\rm MX} = V_{\rm XM}^\dagger$, again with X = L or R.

The definition of the Hamiltonian outlined in this section restricts two-electron interactions to the molecular region. Any physics involving such interactions in the region between molecule and leads is therefore excluded. Such effects, however, can be introduced by redefining the molecule to include the nearest lead atoms. Similarly, interaction between vibrations (phonons) and electronic degrees of freedom can be included in the Hamiltonian, and hence in the MW formula.[12,18] In this paper we restrict ourselves to electron-electron inter-

actions, and this allows us to obtain a strong result about Landauer and non-Landauer contributions to transmission.

2.3 A Green's Function Toolkit

The following section collects useful definitions and relationships.

2.3.1 Definitions

The retarded ($\mathbf{G}^{\mathrm{r}}$) and advanced ($\mathbf{G}^{\mathrm{a}}$) pure-state one-electron GFs are[85]

$$\begin{aligned} G^{\mathrm{r}}_{\mathrm{pq}}(t,t') &= -i\theta(\tau)\langle\{a_{\mathrm{p}}(t), a^{\dagger}_{\mathrm{q}}(t')\}\rangle \\ G^{\mathrm{a}}_{\mathrm{pq}}(t,t') &= \quad i\theta(-\tau)\langle\{a_{\mathrm{p}}(t), a^{\dagger}_{\mathrm{q}}(t')\}\rangle, \end{aligned} \quad (23)$$

where $\tau = t - t'$, $\{a_{\mathrm{p}}, a^{\dagger}_{\mathrm{q}}\}$ is an anti-commutator of destruction (a_{p}) and creation ($a^{\dagger}_{\mathrm{q}}$) operators, and the expectation value is

$$\langle \cdots \rangle = \langle \Psi^N_0 | \cdots | \Psi^N_0 \rangle. \quad (24)$$

The ground state function, $|\Psi^N_0\rangle$, of the N-electron system, satisfies the Schrödinger equation defined with a non-relativistic Born-Oppenheimer many-electron Hamiltonian,

$$H|\Psi^N_0\rangle = E^N_0|\Psi^N_0\rangle, \quad (25)$$

where the ground-state energy is E^N_0. The unit step function is

$$\theta(\tau) = \begin{cases} 1 \text{ for } \tau > 0 \\ 0 \text{ for } \tau \leq 0 \end{cases}. \quad (26)$$

Spin-orbital creation and destruction operators are in the Heisenberg picture,[86]

$$a_{\mathrm{p}}(t) = e^{iHt} a_{\mathrm{p}} e^{-iHt},\ a^{\dagger}_{\mathrm{p}}(t) = e^{iHt} a^{\dagger}_{\mathrm{p}} e^{-iHt}, \quad (27)$$

where the wavefunction is time independent, and the system evolves because the *operators* obey the Heisenberg equation of motion.

Introducing a resolution of the identity inside the operator products in Eq. (23), it is clear that the retarded and advanced GFs depend only upon the time *difference* $\tau = t - t'$. One can introduce energy-dependent GFs by a Fourier transform to give

$$G^{\mathrm{x}}_{\mathrm{pq}}(E) = \int_{-\infty}^{+\infty} e^{iE\tau} e^{-\eta|\tau|} G^{\mathrm{x}}_{\mathrm{pq}}(\tau) d\tau, \quad (28)$$

where x is r or a, and η is a positive infinitesimal used to ensure that the integrand remains finite as $\tau \to \pm\infty$.

The important temperature-dependent generalisations[87] of the definitions in Eq. (23), in which the pure-state average is replaced by a grand canonical ensemble,[27] are not discussed here since they are not used in the present work. We use the Keldysh non-equilibrium GF (NEGF) approach[20–23] which allows the full apparatus of many-body theory to be used for *non-equilibrium* systems. Here, we are not concerned with the details of the preparation of an initial state, so we use a perturbation switched on and off adiabatically at $t = -\infty$, and $t = +\infty$, implying that the theory is defined with respect to the contour defined in Fig. 2. This

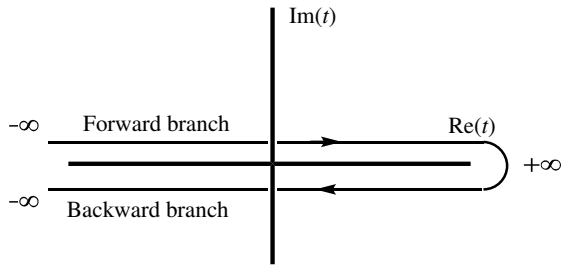

Figure 2: The Keldysh contour, showing forward and backward branches.

two-part contour gives GFs where the ordering of operators is made with respect to their position along the whole contour extending between $-\infty$ and $+\infty$ and back to $-\infty$, and is appropriate for computation of *steady-state* currents. For steady-state systems it can be shown that the NEGFs are invariant to translation in time,[27] i.e. they depend only upon $\tau = t - t'$. Hence, we can define Fourier transform NEGFs through Eq. (28). We use this energy representation of the GFs throughout.

The notation for one-electron NEGFs uses superscripts to distinguish the relative positions of the two times t and t' on the two parts of the Keldysh contour using superscripts. We can de-

fine a *matrix* of GFs as

$$\overline{\mathbf{G}} = \begin{pmatrix} \mathbf{G}^{\mathrm{c}} & \mathbf{G}^{<} \\ \mathbf{G}^{>} & \mathbf{G}^{\widetilde{\mathrm{c}}} \end{pmatrix}. \tag{29}$$

$\mathbf{G}^{\mathrm{c}}$ is the chronological (causal) GF,[85] which has both times on the forward contour:

$$\begin{aligned} G^{\mathrm{c}}_{\mathrm{pq}}(\tau) &= -i\theta(\tau)\langle a_{\mathrm{p}}(t)a^{\dagger}_{\mathrm{q}}(t')\rangle \\ &\quad + i\theta(-\tau)\langle a^{\dagger}_{\mathrm{q}}(t')a_{\mathrm{p}}(t)\rangle \\ &= -i\langle T\left[a_{\mathrm{p}}(t)a^{\dagger}_{\mathrm{q}}(t')\right]\rangle, \end{aligned} \tag{30}$$

where T is the Wick chronological operator that places operators in increasing time order from right to left. $\mathbf{G}^{\widetilde{\mathrm{c}}}$ has both times on the backward contour, so

$$\begin{aligned} G^{\widetilde{\mathrm{c}}}_{\mathrm{pq}}(\tau) &= -i\theta(-\tau)\langle a_{\mathrm{p}}(t)a^{\dagger}_{\mathrm{q}}(t')\rangle \\ &\quad + i\theta(\tau)\langle a^{\dagger}_{\mathrm{q}}(t')a_{\mathrm{p}}(t)\rangle \\ &= -i\langle \widetilde{T}\left[a_{\mathrm{p}}(t)a^{\dagger}_{\mathrm{q}}(t')\right]\rangle, \end{aligned} \tag{31}$$

where $\widetilde{T}$ is the anti-chronological operator, a Wick-like operator that orders time arguments in decreasing time from right to left. The presence of the $\widetilde{T}$ operator emphasises that order *along the contour* is used in the Keldysh definitions, and that time runs in the opposite sense along the backward branch.

The remaining two blocks of Eq. (29) have times on opposite sections of the contour. The lesser GF, $\mathbf{G}^{<}$, has time t on the forward and t' on the backward branch of the contour. The greater GF, $\mathbf{G}^{>}$, has the reverse contour ascription. Hence,

$$\begin{aligned} G^{<}_{\mathrm{pq}}(\tau) &= \quad i\langle a^{\dagger}_{\mathrm{q}}(t')a_{\mathrm{p}}(t)\rangle, \\ G^{>}_{\mathrm{pq}}(\tau) &= -i\langle a_{\mathrm{p}}(t)a^{\dagger}_{\mathrm{q}}(t')\rangle. \end{aligned} \tag{32}$$

2.3.2 Dyson Equations

Equilibrium and non-equilibrium two-time GFs, $\mathbf{G}$, satisfy Dyson equations, which are derived using time-dependent perturbation theory to express the exact GF in terms of a zeroth-order GF for which we shall use a lower-case notation, $\mathbf{g}$. Each of these component GFs is defined with respect to basis orbitals for a part of the device, i.e. the leads, L and R, or the molecule, M. The GF matrix blocks are labelled accordingly, so that $\mathbf{G}^{<}_{\mathrm{ML}}$, is a matrix block with rows referring to the molecule, and columns to lead L.

The zeroth-order GFs describe an equilibrium system with no coupling between the leads and the molecule, and $\mathbf{g}^{\mathrm{x}}_{\mathrm{LL}}$, $\mathbf{g}^{\mathrm{x}}_{\mathrm{MM}}$, and $\mathbf{g}^{\mathrm{x}}_{\mathrm{RR}}$ are lead L, molecule M, and lead R GFs, respectively, with x = r, a, >, etc.

The Dyson equation allows dressed GFs, $\mathbf{G}^{\mathrm{x}}$, to be expressed in terms of zeroth-order undressed GFs, $\mathbf{g}^{\mathrm{x}}$, as

$$\mathbf{G}^{\mathrm{x}} = \mathbf{g}^{\mathrm{x}} + \mathbf{g}^{\mathrm{x}}\mathbf{\Sigma}^{\mathrm{x}}\mathbf{G}^{\mathrm{x}}, \text{ where } x = r, a, \tag{33}$$

where the self-energy, $\mathbf{\Sigma}$, contains the effects of the perturbation through all orders, and each term is implicitly E-dependent. Using matrix algebra, this equation can be recast as

$$(\mathbf{g}^{\mathrm{x}})^{-1}\mathbf{G}^{\mathrm{x}} = \mathbf{1} + \mathbf{\Sigma}^{\mathrm{x}}\mathbf{G}^{\mathrm{x}}, \tag{34}$$

or the inverse form

$$(\mathbf{G}^{\mathrm{x}})^{-1} = (\mathbf{g}^{\mathrm{x}})^{-1} - \mathbf{\Sigma}^{\mathrm{x}}. \tag{35}$$

For NEGFs, the Dyson equation retains the form of Eq. (33) *provided* we use the whole matrix $\overline{\mathbf{G}}(E)$. To obtain an equation for a single block, such as $\mathbf{G}^{<}$, it is necessary to separate out the different Keldysh contour blocks using matrix multiplication. This gives the more complicated Keldysh equation,[12,27]

$$\mathbf{G}^{<} = (\mathbf{1} + \mathbf{G}^{\mathrm{r}}\mathbf{\Sigma}^{\mathrm{r}})\,\mathbf{g}^{<}\,(\mathbf{1} + \mathbf{\Sigma}^{\mathrm{a}}\mathbf{G}^{\mathrm{a}}) + \mathbf{G}^{\mathrm{r}}\mathbf{\Sigma}^{<}\mathbf{G}^{\mathrm{a}}. \tag{36}$$

By using Eq. (34) and its adjoint this equation simplifies to the product form

$$\mathbf{G}^{<} = \mathbf{G}^{\mathrm{r}}\left[(\mathbf{g}^{\mathrm{r}})^{-1}\mathbf{g}^{<}(\mathbf{g}^{\mathrm{a}})^{-1} + \mathbf{\Sigma}^{<}\right]\mathbf{G}^{\mathrm{a}}. \tag{37}$$

2.3.3 The Embedding Self-energy

The perturbation theory for a molecular device is defined in terms of the one-electron interaction, $\mathbf{V}$, in Eq. (21). Using matrix block multiplication, it follows that for x = r, a, the molecular block of Dyson's equation is

$$\mathbf{G}^{x}_{\mathrm{MM}} = \mathbf{g}^{x}_{\mathrm{MM}} + \sum_{\mathrm{X=L,R}} \mathbf{g}^{x}_{\mathrm{MM}}\mathbf{V}_{\mathrm{MX}}\mathbf{G}^{x}_{\mathrm{XM}}, \tag{38}$$

and off-diagonal blocks are

$$\mathbf{G}^{x}_{\mathrm{XM}} = \mathbf{g}^{x}_{\mathrm{XX}}\mathbf{V}_{\mathrm{XM}}\mathbf{G}^{x}_{\mathrm{MM}}, \text{ for } \mathrm{X} = \mathrm{L}, \mathrm{R}, \quad (39)$$

using the block-diagonal nature of the zeroth-order GFs. Substitution of Eq. (39) into Eq. (38) leads to a Dyson equation for the molecular GF[12,27]

$$\mathbf{G}^{\mathrm{x}}_{\mathrm{MM}} = \mathbf{g}^{\mathrm{x}}_{\mathrm{MM}} + \mathbf{g}^{\mathrm{x}}_{\mathrm{MM}}\mathbf{\Omega}^{\mathrm{x}}_{\mathrm{MM}}\mathbf{G}^{\mathrm{x}}_{\mathrm{MM}}, \quad (40)$$

where the embedding self-energy is

$$\begin{aligned}\mathbf{\Omega}^{\mathrm{x}}_{\mathrm{MM}} &= \mathbf{\Omega}^{\mathrm{x,L}}_{\mathrm{MM}} + \mathbf{\Omega}^{\mathrm{x,R}}_{\mathrm{MM}},\\ \mathbf{\Omega}^{\mathrm{x,X}}_{\mathrm{MM}} &= \mathbf{V}_{\mathrm{MX}}\mathbf{g}^{\mathrm{x}}_{\mathrm{XX}}\mathbf{V}_{\mathrm{XM}}, \text{ for } \mathrm{X} = \mathrm{L}, \mathrm{R}. \end{aligned} \quad (41)$$

Scattering rate matrices can now be defined (see Ref. 27, p. 266) as

$$\Gamma^{\mathrm{X}}_{\mathrm{MM}} = i\Delta\mathbf{\Omega}^{\mathrm{X}}_{\mathrm{MM}} \text{ for } \mathrm{X} = \mathrm{L}, \mathrm{R}. \quad (42)$$

2.3.4 The Correlation Self-energy

Although the molecular GF, $\mathbf{g}_{\mathrm{MM}}$, is of zeroth order in terms of the device perturbation, $\mathbf{V}$, it is the *exact* GF for a correlated molecule. It can be expanded as a perturbation series in terms of electron correlation.[86] The Dyson equation reads

$$\mathbf{g}^{\mathrm{x}}_{\mathrm{MM}} = \mathbf{g}^{\mathrm{HF,x}}_{\mathrm{MM}} + \mathbf{g}^{\mathrm{HF,x}}_{\mathrm{MM}}\mathbf{M}^{\mathrm{x}}_{\mathrm{MM}}\mathbf{g}^{\mathrm{x}}_{\mathrm{MM}}, \quad (43)$$

where $\mathrm{x} = \mathrm{r}, \mathrm{a}$, and $\mathbf{M}$ is the electron correlation self-energy and $\mathbf{g}^{\mathrm{HF,x}}_{\mathrm{MM}}$ is the Hartree-Fock (HF) GF. The retarded and advanced HF GFs are[12]

$$(\mathbf{g}^{\mathrm{HF,r,a}}_{\mathrm{MM}})_{\mathrm{pq}} = \delta_{\mathrm{pq}}(\mathcal{E}^{\mathrm{r,a}} - \epsilon_{\mathrm{p}})^{-1}, \quad (44)$$

where ϵ_{p} are HF orbital energies, $\mathcal{E}^{\mathrm{r,a}} = E \pm i\eta$, and η is a positive infinitesimal.

The simplest approximation to $\mathbf{M}$ comes from second-order perturbation theory,[86] and is expressed in terms of HF spinorbitals and orbital energies as

$$\begin{aligned}\mathbf{M}^{\mathrm{x},(2)}_{\mathrm{pq}} = &\frac{1}{2}\sum_{\mathrm{ija}}\frac{\langle \mathrm{pa}||\mathrm{ij}\rangle\langle \mathrm{ij}||\mathrm{aq}\rangle}{\mathcal{E}^{\mathrm{x}} - \epsilon_{\mathrm{ija}}}\\ &+ \frac{1}{2}\sum_{\mathrm{abi}}\frac{\langle \mathrm{pi}||\mathrm{ab}\rangle\langle \mathrm{ab}||\mathrm{iq}\rangle}{\mathcal{E}^{\mathrm{x}} - \epsilon_{\mathrm{abi}}}, \end{aligned} \quad (45)$$

where

$$\epsilon_{\mathrm{pqr}} = \epsilon_{\mathrm{p}} + \epsilon_{\mathrm{q}} - \epsilon_{\mathrm{r}}. \quad (46)$$

The inverse form of the Dyson equation (see Eq. (35)) can be used twice to give

$$\begin{aligned}(\mathbf{G}^{\mathrm{x}}_{\mathrm{MM}})^{-1} &= (\mathbf{g}^{\mathrm{x}}_{\mathrm{MM}})^{-1} - \mathbf{\Omega}^{\mathrm{x}}_{\mathrm{MM}},\\ &= (\mathbf{g}^{\mathrm{HF,x}}_{\mathrm{MM}})^{-1} - \mathbf{\Omega}^{\mathrm{x}}_{\mathrm{MM}} - \mathbf{M}^{\mathrm{x}}_{\mathrm{MM}} \end{aligned} \quad (47)$$

The MW formula in Eq. (6) includes the quantity $\Delta\mathbf{G}_{\mathrm{MM}}$ defined in Eq. (7), which can also be simplified using the inverse form of the Dyson equation:

$$\begin{aligned}\Delta\mathbf{G}_{\mathrm{MM}} &= \mathbf{G}^{\mathrm{r}}_{\mathrm{MM}}\left[(\mathbf{G}^{\mathrm{a}}_{\mathrm{MM}})^{-1} - (\mathbf{G}^{\mathrm{r}}_{\mathrm{MM}})^{-1}\right]\mathbf{G}^{\mathrm{a}}_{\mathrm{MM}}\\ &= \mathbf{G}^{\mathrm{r}}_{\mathrm{MM}}\Big[(\mathbf{g}^{\mathrm{HF,a}}_{\mathrm{MM}})^{-1} - \mathbf{M}^{\mathrm{a}}_{\mathrm{MM}} - \mathbf{\Omega}^{\mathrm{a}}_{\mathrm{MM}}\\ &\quad - (\mathbf{g}^{\mathrm{HF,r}}_{\mathrm{MM}})^{-1} + \mathbf{M}^{\mathrm{r}}_{\mathrm{MM}} + \mathbf{\Omega}^{\mathrm{r}}_{\mathrm{MM}}\Big]\mathbf{G}^{\mathrm{a}}_{\mathrm{MM}}. \end{aligned} \quad (48)$$

Using Eq. (44) and the definition of $\mathcal{E}^{x}$ it follows that

$$(\mathbf{g}^{\mathrm{HF,r}}_{\mathrm{MM}})^{-1} - (\mathbf{g}^{\mathrm{HF,a}}_{\mathrm{MM}})^{-1} = 2i\eta\mathbf{1} = \mathbf{0}, \quad (49)$$

and hence we have again a product form

$$\Delta\mathbf{G}_{\mathrm{MM}} = \mathbf{G}^{\mathrm{r}}_{\mathrm{MM}}\left[\Delta\mathbf{\Omega}_{\mathrm{MM}} + \Delta\mathbf{M}_{\mathrm{MM}}\right]\mathbf{G}^{\mathrm{a}}_{\mathrm{MM}}. \quad (50)$$

The lesser GF, $\mathbf{G}^{<}_{\mathrm{MM}}$, can also be simplified, using the Keldysh equation in the form of Eq. (37) to give

$$\mathbf{G}^{<}_{\mathrm{MM}} = \sum_{\mathrm{X}}\mathbf{G}^{\mathrm{r}}_{\mathrm{MX}}(\mathbf{g}^{\mathrm{r}}_{\mathrm{XX}})^{-1}\mathbf{g}^{<}_{\mathrm{XX}}(\mathbf{g}^{\mathrm{a}}_{\mathrm{XX}})^{-1}\mathbf{G}^{\mathrm{a}}_{\mathrm{XM}}, \quad (51)$$

where we have used the fact that $\mathbf{\Sigma}^{<} = \mathbf{0}$ for the one-electron perturbation $\mathbf{V}$, because one-electron operators carry a single time-point in the time-dependent perturbation theory (see Ref. 12, p. 185, Eq. (7.23)).

All the zeroth-order NEGFs, $\mathbf{g}^{<}_{\mathrm{XX}}$, describe equilibrium electron distributions, and therefore satisfy the fluctuation-dissipation theorem (see Ref. 27, p. 177)

$$\mathbf{g}^{<}_{\mathrm{XX}} = -f_{\mathrm{X}}(\mathbf{g}^{\mathrm{r}}_{\mathrm{XX}} - \mathbf{g}^{\mathrm{a}}_{\mathrm{XX}}) = f_{\mathrm{X}}\Delta\mathbf{g}_{\mathrm{XX}}, \quad (52)$$

which is true for the interacting-electron GF, $\mathbf{g}^<_{\rm MM}$, as well as its non-interacting lead counterparts. The X = M term of Eq. (51) can be simplified using Eq. (52), and the Dyson equation Eq. (43) in the inverse form, Eq. (35), to give

$$(\mathbf{g}^{\rm r}_{\rm MM})^{-1}\mathbf{g}^<_{\rm MM}(\mathbf{g}^{\rm a}_{\rm MM})^{-1} = -f_{\rm M}\Delta\mathbf{M}. \qquad (53)$$

For the lead block contributions to Eq. (51), we use Eq. (39) and its adjoint, so that it can be simplified using Eq. (52) and the Dyson equation in the inverse form, Eq. (35), to give

$$\mathbf{G}^{\rm r}_{\rm MX}(\mathbf{g}^{\rm r}_{\rm XX})^{-1}\mathbf{g}^<_{\rm XX}(\mathbf{g}^{\rm a}_{\rm XX})^{-1}\mathbf{G}^{\rm a}_{\rm XM} = -f_{\rm X}\mathbf{G}^{\rm r}_{\rm MM}\Delta\Omega^{\rm X}_{\rm MM}\mathbf{G}^{\rm a}_{\rm MM}, \text{ for X} = \text{L or R}. \qquad (54)$$

Finally, collecting all the terms together,

$$\mathbf{G}^<_{\rm MM} = -\,\mathbf{G}^{\rm r}_{\rm MM}\left(f_{\rm L}\Delta\mathbf{\Omega}^{\rm L}_{\rm MM} + f_{\rm R}\Delta\mathbf{\Omega}^{\rm R}_{\rm MM} + f_{\rm M}\Delta\mathbf{M}_{\rm MM}\right)\mathbf{G}^{\rm a}_{\rm MM}. \qquad (55)$$

To emphasise, this expression has been derived using only the Keldysh equation, Eq. (36), and matrix partitioning in terms of the blocks L, R and M.

We now have all the necessary quantities expressed in terms of retarded and advanced GFs and self-energies, allowing us make a simple partition of the MW formula.

2.4 The Meir-Wingreen formula

The MW formula,[19] Eq. (6), for the steady-state current was derived using NEGF techniques,[20–23] and is exact for interacting systems. It was derived using the same zeroth-order starting point as the present paper. To be explicit, the zeroth-order molecular GF is fully correlated. Eq. (6) can be simplified using Eqs. (50) and (55) to give

$$J_{\rm L\sigma} = \frac{i}{2\pi}\int dE\,{\rm tr}\,\mathbf{\Gamma}^{\rm L}_{\rm MM}\mathbf{G}^{\rm r}_{\rm MM}\Big\{(f_{\rm L}-f_{\rm R})\Delta\mathbf{\Omega}^{\rm R}_{\rm MM} + (f_{\rm L}-f_{\rm M})\Delta\mathbf{M}_{\rm MM}\Big\}\mathbf{G}^{\rm a}_{\rm MM}. \qquad (56)$$

This expression depends on distinct self-energies, the embedding self-energy, $\mathbf{\Omega}$, arising from the lead-molecule interaction, and the correlation self-energy, $\mathbf{M}$, arising from the electron-electron interactions. These describe physically distinct effects. This enables a partition of Eq. (56) into the Landauer and non-Landauer terms described below. This partition was first noted by Caroli,[18] (for details see Ref. 12, p. 216, Eqs. (8.34) and (8.35)) in the context of electron-phonon interactions.

2.4.1 The Landauer Current

The *Landauer* current, depends directly on the scattering rate matrix for lead L. It describes the *elastic* scattering of a particle (or hole) by the lead-molecule interactions without exchange of energy with the molecule. Using Eqs. (41), (52) and (42), and using the definition of the rate matrices in Eq. (42), the *total elastic current*, $J^{\rm LB}$, is found to be (in a.u.)

$$J^{\rm LB}_{\rm L\sigma} = \frac{1}{2\pi}\int_{-\infty}^{+\infty}(f_{\rm L}-f_{\rm R})\,T^{\rm LB}_{\rm L\sigma}dE, \qquad (57)$$

where the expression for the elastic transmission,

$$T^{\rm LB}_{\rm L\sigma} = {\rm tr}\mathbf{G}^{\rm r}_{\rm MM}\mathbf{\Gamma}^{\rm L}_{\rm MM}\mathbf{G}^{\rm a}_{\rm MM}\mathbf{\Gamma}^{\rm R}_{\rm MM}, \qquad (58)$$

is a *correlated* Landauer-Büttiker formula. It is identical in form to the uncorrelated expression in Eq. (3). The dressed GF, $\mathbf{G}^{\rm r,a}_{\rm MM}$, however, now contains the effects of *molecular* electron correlation (in principle to all orders). It also contains the molecule-lead interaction to all orders.

The NEGF method makes no distinction between source and sink leads. The direction of current flow is determined solely by the difference in the distribution functions, $f_{\rm L}$ and $f_{\rm R}$. Clearly $T^{\rm LB}_{\rm L\sigma}$ is symmetric in lead labels, and $J^{\rm LB}_{\rm R\sigma}$ can be derived by exchanging them. Hence,

$$J^{\rm LB}_{\rm L\sigma} + J^{\rm LB}_{\rm R\sigma} = 0, \qquad (59)$$

so that total elastic current *into* the molecule from the two leads is zero, which is equivalent to Kirchhoff conservation.

2.4.2 The non-Landauer Current

The *non-Landauer* current, J^{nonLB},

$$J^{\mathrm{nonLB}}_{\mathrm{L}\sigma} = \frac{i}{2\pi}\int dE \mathrm{tr}\boldsymbol{\Gamma}^{\mathrm{L}}_{\mathrm{MM}}\mathbf{G}^{\mathrm{r}}_{\mathrm{MM}}\times (f_{\mathrm{L}} - f_{\mathrm{M}})\,\Delta\mathbf{M}_{\mathrm{MM}}\mathbf{G}^{\mathrm{a}}_{\mathrm{MM}}, \qquad (60)$$

depends directly upon the correlation self-energy.

The correlation self-energy, $\mathbf{M}_{\mathrm{MM}}(E)$, involves propagation of a particle (or hole) together with electron excitation (or de-excitation), so that energy is lost from (or gained by) the electron beam. In the steady state approximation, the energy lost by excitation must be balanced by energy gained by de-excitation, and we might therefore expect this term to be zero, as will now be proved.

It is a striking fact that the analytical form of the *exact* retarded/advanced correlation self-energy has been known. It is[88–90]

$$\mathbf{M}^{x}(E) = \mathbf{M}^{\infty} + \mathbf{M}^{h}(\mathcal{E}^{x}) + \mathbf{M}^{p}(\mathcal{E}^{x}), \qquad (61)$$

where

$$M^{\infty}_{\mathrm{pq}} = \lim_{E\to\infty} M^{x}_{\mathrm{pq}}(E) = F_{\mathrm{pq}}(\rho_1 - \rho_1^{\mathrm{HF}}) \qquad (62)$$

is a Hermitian static term accounting for the change in the density-dependent Fock operator, $F(\rho)$, on going from the Hartree-Fock density to the exact one-density. The energy-dependent hole and particle terms are

$$M^{h}_{\mathrm{pq}}(\mathcal{E}^{x}) = \sum_{\mathrm{i}} \frac{\mathcal{X}_{\mathrm{pi}}\mathcal{X}^{*}_{\mathrm{qi}}}{\mathcal{E}^{x} - \Lambda_{\mathrm{i}}},$$
$$M^{p}_{\mathrm{pq}}(\mathcal{E}^{x}) = \sum_{\mathrm{a}} \frac{\mathcal{Y}_{\mathrm{pa}}\mathcal{Y}^{*}_{\mathrm{qa}}}{\mathcal{E}^{x} - \Lambda_{\mathrm{a}}}, \qquad (63)$$

which are expressions analogous to the Lehmann expansion of the GF (see Eq. (99)). In the present case, however, the Dyson-like orbital coefficients, $\mathcal{X}_{\mathrm{pi}}$, $\mathcal{Y}_{\mathrm{pa}}$, and the poles Λ_{i}, Λ_{a}, cannot be identified in terms of the exact states of the molecular system. We can easily deduce that

$$\Delta M_{\mathrm{pq}} = \frac{\pi}{2i}\left\{\sum_{\mathrm{i}} \mathcal{X}_{\mathrm{pi}}\mathcal{X}^{*}_{\mathrm{qi}}\delta(E-\Lambda_{\mathrm{i}}) + \sum_{\mathrm{i}} \mathcal{Y}_{\mathrm{pa}}\mathcal{Y}^{*}_{\mathrm{qa}}\delta(E-\Lambda_{\mathrm{a}})\right\}, \qquad (64)$$

has Dirac delta function contributions at each pole of the correlation self energy. It is obvious from Eq. (47), that the poles of the self-energy are the zeroes of $\mathbf{G}$, which implies in turn that the non-Landauer current, J^{nonLB}, is indeed zero.

Thus, there are *no* non-Landauer terms arising from electron-electron interactions in the current model. This is not the case when electron-phonon interactions are included in the Hamiltonian. Such interactions couple electron and phonon GFs, producing terms in which energy is passed to (and from) the molecule into the phonon modes. These interactions are important in some experimental contexts, for example in the study of vibronic effects in MEDs via the IELTS technique.[8] It should be noted that for electron-phonon interactions, the non-Landauer term is usually called the 'inelastic scattering' term. Such nomenclature seems less appropriate for electron-electron interactions. In our treatment, the term vanishes.

Computations of molecular conduction using the GF formalism must, of necessity, use approximate forms for the self-energy. Not all approximation schemes reproduce the form shown in Eq. (61). The methodologies known to satisfy this requirement include the second-order GF, the 2ph Tamm-Dancoff approximation,[91,92] and a range of algebraic diagrammatic construction approaches due to Cederbaum et al.[88] Approximations that respect the form of the correlation self-energy guarantee that the calculated electron current is symmetrical in terms of the leads. There is no need for any ad hoc symmetrisation of the MW formula in this case.

2.5 Comparing NEGF and SSP

This section postulates an *Ansatz* for a Source-Sink-Potential (SSP) method that differs in two

ways from the standard formulation.[73] It allows a more general connection between leads and molecule. It also includes the effects of molecular electron correlation. We use it to explore the relationship between the NEGF and SSP approaches for correlated molecules.

2.5.1 The uncorrelated SSP method

The conventional SSP method[51,52,63,77,93–100] assumes a tight-binding (Hückel) representation for the whole device. In our recent reformulation,[73] we define scattering wavefunctions in source (L) and in sink (R) leads as

$$\psi^{\mathrm{L}} = \sum_{\mathrm{p}\in\mathrm{L}} c_{\mathrm{p}}^{\mathrm{L}}\phi_{\mathrm{p}},\ \psi^{\mathrm{R}} = \sum_{\mathrm{p}\in\mathrm{R}} c_{\mathrm{p}}^{\mathrm{R}}\phi_{\mathrm{p}}, \tag{65}$$

where the coefficients

$$c_{\mathrm{p}}^{\mathrm{L}} = \frac{1}{N_{\mathrm{L}}}(e^{-iq_{\mathrm{L}}\mathrm{p}} + re^{iq_{\mathrm{L}}\mathrm{p}}),\ c_{\mathrm{p}}^{\mathrm{R}} = \frac{\tau}{N_{\mathrm{R}}}e^{iq_{\mathrm{R}}\mathrm{p}}, \tag{66}$$

provide the boundary conditions for *elastic* scattering.

The source wavefunction, ψ^{L}, is a combination of a forward travelling wave (i.e. towards the right in Fig. 1a, in the direction of decreasing atom number), and a reflected wave, with wavevectors $-q_{\mathrm{L}}$ and q_{L} respectively. The reflected wave arises from scattering from the molecule with reflection coefficient, r. The sink lead has a forward-travelling wave component with wavevector q_{R} and transmission coefficient τ. Normalisation constants, N_{L} and N_{R}, are determined such that each wire transmits one electron with spin σ. This leads to[73]

$$N_{\mathrm{L}}^2 = 2\beta_{\mathrm{L}}\sin q_{\mathrm{L}},\ N_{\mathrm{R}}^2 = 2\beta_{\mathrm{R}}\sin q_{\mathrm{R}}. \tag{67}$$

Eqs. (65), (66) and (67) imply that

$$0 \le T_{\mathrm{L}\sigma}^{\mathrm{SSP}} = 1 - |r|^2 = |\tau|^2 = T_{\mathrm{R}\sigma}^{\mathrm{SSP}} \le 1. \tag{68}$$

We now assume that atoms 1 to n_{L} in lead L, and 1 to n_R in lead R, have multiple contacts with the molecule, as shown in Fig. 1a. The secular equation for the outermost atom in lead L interacting with the molecule (n_{L}, in Fig. 1) is

$$-\beta_{\mathrm{L}}(c_{n_{\mathrm{L}}+1}^{\mathrm{L}} + c_{n_{\mathrm{L}}-1}^{\mathrm{L}}) + (E-\alpha_{\mathrm{L}})\,c_{n_{\mathrm{L}}}^{\mathrm{L}} - \sum_{\mathrm{p}\in\mathrm{M}}(\mathrm{V}_{\mathrm{LM}})_{n_{\mathrm{L}}\mathrm{p}}c_{\mathrm{p}} = 0. \tag{69}$$

The aim of the SSP method is to replace the semi-infinite lead with a finite lead truncated at atom n_{L} (and atom n_{R} in lead R), as shown in Fig. 1b. The outer terminal atoms become the source and sink for current in the device. To achieve this, we eliminate $c_{n_{\mathrm{L}}+1}^{\mathrm{L}}$ using Eq. (66),

$$c_{n_{\mathrm{L}}+1}^{\mathrm{L}} = \frac{1}{N_{\mathrm{L}}}\left(e^{-i(n_{\mathrm{L}}+1)q_{\mathrm{L}}} + re^{i(n_{\mathrm{L}}+1)q_{\mathrm{L}}}\right). \tag{70}$$

The unknown quantity r can be expressed in terms of the coefficient $c_{n_{\mathrm{L}}}^{\mathrm{L}}$, using Eq. (66) again, as

$$r = e^{-in_{\mathrm{L}}q_{\mathrm{L}}}(N_{\mathrm{L}}c_{n_{\mathrm{L}}}^{\mathrm{L}} - e^{-in_{\mathrm{L}}q_{\mathrm{L}}}). \tag{71}$$

Substituting these two equations into Eq. (69),

$$\begin{aligned}(E-\ \alpha_{\mathrm{L}} - \beta_{\mathrm{L}}e^{iq_{\mathrm{L}}})\,c_{n_{\mathrm{L}}}^{\mathrm{L}} - \beta_{\mathrm{L}}c_{n_{\mathrm{L}}-1}^{\mathrm{L}} &- \sum_{\mathrm{p}\in\mathrm{M}}(\mathrm{V}_{\mathrm{LM}})_{n_{\mathrm{L}}\mathrm{p}}c_{\mathrm{p}} \\ &= -\frac{2i\beta_{\mathrm{L}}\sin q_{\mathrm{L}}}{N_{\mathrm{L}}}e^{-in_{\mathrm{L}}q_{\mathrm{L}}} \\ &= -iN_{\mathrm{L}}e^{-in_{\mathrm{L}}q_{\mathrm{L}}},\end{aligned} \tag{72}$$

where the inhomogeneous term has been moved to the right-hand side. The secular equations are truncated at atom n_{L}: for lead atoms *closer* to the molecule, the standard Hückel secular equations for a chain of length n_{L} apply.

The source term in Eq. (72) manifests in two ways. First, there is the inhomogeneity, which can be thought of as equivalent to the boundary condition for an incoming elastic scattered wave in lead L such that Eq. (68) is satisfied. Secondly, the matrix element multiplying $c_{n_{\mathrm{L}}}^{\mathrm{L}}$ becomes

$$E - \alpha_{\mathrm{L}} - \beta_{\mathrm{L}}e^{iq_{\mathrm{L}}} = \beta_{\mathrm{L}}e^{-iq_{\mathrm{L}}}, \tag{73}$$

where we have used the Hückel dispersion relations (of Eq. (13)). The result is that all atoms to the left of n_{L} are replaced by a *complex* potential, $\beta_{\mathrm{L}}e^{iq_{\mathrm{L}}}$, on atom n_{L}, the *source potential*,

a non-Hermitian term that creates the incoming current.

The secular equation for the terminal atom on lead R can be treated in the same way. In this case, there is no inhomogeneous term because only a transmitted wave exists in the sink lead, and

$$c_{n_{\rm R}} = \tau e^{in_{\rm L}q_{\rm R}}, \tag{74}$$

so that τ can be expressed simply in terms of the coefficient on the outermost contact atom, $n_{\rm R}$ in the right-hand lead. The secular equations for lead R are similarly derived, and the diagonal interaction on atom $n_{\rm R}$ becomes

$$E - \alpha_{\rm R} - \beta_{\rm R}e^{iq_{\rm R}} = \beta_{\rm R}e^{-iq_{\rm R}}. \tag{75}$$

We conclude that the *uncorrelated* SSP equations are

$$\mathbf{P}_{\rm SSP}\begin{pmatrix}\mathbf{c}_{\rm M}\\ \mathbf{c}_{\rm L}\\ \mathbf{c}_{\rm R}\end{pmatrix} = \begin{pmatrix}\mathbf{0}\\ \mathbf{b}_{\rm L}\\ 0\end{pmatrix}, \tag{76}$$

where the inhomogeneous term, $\mathbf{b}_{\rm L}$, has a single non-zero element (corresponding to the source):

$$(\mathbf{b}_{\rm L})_{\rm p} = \delta_{p,n_{\rm L}}(-iN_{\rm L}e^{-in_{\rm L}q_{\rm L}}). \tag{77}$$

The SSP device matrix is

$$\mathbf{P}_{\rm SSP} = \begin{pmatrix}E\mathbf{1}-\mathbf{h}_{\rm M} & -\mathbf{V}_{\rm ML} & -\mathbf{V}_{\rm MR}\\ -\mathbf{V}_{\rm LM} & E\mathbf{1}-\mathbf{h}_{\rm L} & 0\\ -\mathbf{V}_{\rm RM} & 0 & E\mathbf{1}-\mathbf{h}_{\rm R}\end{pmatrix}. \tag{78}$$

where the matrices $\mathbf{h}^{\rm M}$, $\mathbf{h}^{\rm L}$, and $\mathbf{h}^{\rm R}$ are Hückel Hamiltonian matrices for the various parts of the SSP device, including the extra source and sink complex potentials implied by Eqs. (73), and (75). The components of the device vector $\mathbf{c}_{\rm M}$, $\mathbf{c}_{\rm L}$, and $\mathbf{c}_{\rm R}$ specify the device wavefunction in terms of basis functions on the molecule and source and sink atoms.

We can use the expressions for the coefficients $c_{n_{\rm L}}$ and $c_{n_{\rm R}}$ in Eq. (66) to show that

$$\begin{aligned} T^{\rm SSP}_{{\rm L}\sigma} &= 1-|r|^2 = N_{\rm L}(c_{n_{\rm L}}+c^*_{n_{\rm L}}) - N_{\rm L}^2|c_{n_{\rm L}}|^2,\\ T^{\rm SSP}_{{\rm R}\sigma} &= |\tau|^2 = N_{\rm R}^2|c_{n_{\rm R}}|^2. \end{aligned} \tag{79}$$

Hence, solution of the SSP matrix equation, Eq. (76), yields SSP coefficients which can be used via Eq. (79) to give the transmission. Eqs. (76) and (78) give the essence of the uncorrelated SSP model for a device with multiple contacts between leads and molecule. They are now ready to be modified to include electron correlation.

2.5.2 Correlated SSP

The Hückel SSP device matrix Eq. (78) can also be written in terms of undressed GFs in the form

$$\mathbf{P}_{\rm SSP} = \begin{pmatrix}(\mathbf{g}^{\rm r,H\ddot{u}ck}_{\rm MM})^{-1} & -\mathbf{V}_{\rm ML} & -\mathbf{V}_{\rm MR}\\ -\mathbf{V}_{\rm LM} & (\bar{\mathbf{g}}^{\rm r}_{\rm LL})^{-1} & 0\\ -\mathbf{V}_{\rm RM} & 0 & (\bar{\mathbf{g}}^{\rm r}_{\rm RR})^{-1}\end{pmatrix}, \tag{80}$$

Here, we have used Eq. (16) to identify the Hückel molecular GF.

Retarded/advanced GFs for semi-infinite leads can be expressed analytically[12,101] in terms of the wavevector, $q_{\rm X}$, as

$$(g^{\rm x}_{\rm XX})_{\rm pp'} = \frac{e^{\pm i{\rm p}_> q_{\rm X}}}{\beta_{\rm X}}\frac{\sin({\rm p}_< q_{\rm X})}{\sin q_{\rm X}} \tag{81}$$

where X = L or R, and $\rm p_>$ and $\rm p_<$ are the larger and smaller of the atom labels p and p′, respectively, for the general connection in Fig. 1a.

The matrix $(\bar{\mathbf{g}}^{\rm r}_{\rm LL})^{-1}$ can be deduced directly from the SSP secular equations derived in the previous section, i.e.

$$(\bar{\mathbf{g}}^{\rm r}_{\rm LL})^{-1} = \begin{pmatrix}\mathcal{E}^{\rm r}\mathbf{1}-\mathbf{h}^{\rm H\ddot{u}ck} & \mathbf{0}\\ \mathbf{0} & \beta_{\rm L}e^{-iq_{\rm L}}\end{pmatrix}. \tag{82}$$

We use the analogous definition for $\bar{\mathbf{g}}^{\rm r}_{\rm RR}$. The inverse of $(\bar{\mathbf{g}}^{\rm r}_{\rm LL})^{-1}$ reproduces the expression in Eq. (81), so the bar indicates that we are using the inverse of the $n_{\rm L}\times n_{\rm L}$ block of $\mathbf{g}^{\rm r}_{\rm LL}$, rather than the inverse of the infinite-dimensional matrix. The specification of *retarded* GFs in Eq. (80) arises from the sign of the complex terms in source and sink potentials.

For the correlated version of the SSP equation

we make the obvious *Ansatz*

$$\mathbf{P}^{\rm corr}_{\rm SSP} = \begin{pmatrix} (\mathbf{g}^{\rm r}_{\rm MM})^{-1} & -\mathbf{V}_{\rm ML} & -\mathbf{V}_{\rm MR} \\ -\mathbf{V}_{\rm LM} & (\bar{\mathbf{g}}^{\rm r}_{\rm LL})^{-1} & 0 \\ -\mathbf{V}_{\rm RM} & 0 & (\bar{\mathbf{g}}^{\rm r}_{\rm RR})^{-1}. \end{pmatrix}, \tag{83}$$

where $\mathbf{g}^{\rm r}_{\rm MM}$ is the *correlated* GF for the isolated molecule (i.e. without interaction with the leads), and the distinction between retarded and advanced GF could be suppressed for reasons already noted.

Finally, the correlated SSP equation is

$$\mathbf{P}^{\rm corr}_{\rm SSP} \begin{pmatrix} \mathbf{c}_{\rm M} \\ \mathbf{c}_{\rm L} \\ \mathbf{c}_{\rm R} \end{pmatrix} = \begin{pmatrix} \mathbf{0} \\ \mathbf{b}_{\rm L} \\ \mathbf{0} \end{pmatrix}, \tag{84}$$

where the $n_{\rm L} \times 1$ element column vector, $\mathbf{b}_{\rm L}$, is a source term to be determined subsequently. We emphasise here that the entries, $\mathbf{c}(E)$, in the correlated solution vector are for an SSP *elastic-scattering* device at energy, E. The interpretation of the $\mathbf{c}$ coefficients will emerge: they represent the composition of a device wavefunction that gives transmission consistent with the MW equation.

To summarise, Eq. (84) is the form of the SSP equation extended to include electron correlation, consistent with the MW approach, and retaining the interpretive advantages of the SSP method.

2.5.3 Equivalence of SSP and MW

To solve the correlated SSP equation, Eq. (84), we need the inverse, $(\mathbf{P}^{\rm corr}_{\rm SSP})^{-1}$. Eq. (83) can be written as an inverse Dyson equation in the style of Eq. (47):

$$\mathbf{P}^{\rm corr}_{\rm SSP} = (\mathbf{g}^{\rm r})^{-1} - \mathbf{V} = (\mathbf{G}^{\rm r})^{-1}, \tag{85}$$

where $(\mathbf{g}^{\rm r})^{-1}$ is the block diagonal part of $\mathbf{P}$.

The dressed GF, $\mathbf{G}^{\rm r}$, has a physical significance. Its poles are complex-valued, representing device resonances corresponding to the presence of an extra electron or hole in the sea of correlated electrons. The imaginary parts of these poles are inversely related to the lifetimes of the resonances. We conclude that these lifetimes represent transit times for the particles or holes crossing the device.

The SSP solution vector follows from Eq. (85) as

$$\mathbf{c}_{\rm M} = \mathbf{G}^{\rm r}_{\rm ML}\mathbf{b}_{\rm L},\ \mathbf{c}_{\rm L} = \mathbf{G}^{\rm r}_{\rm LL}\mathbf{b}_{\rm L},\ \mathbf{c}_{\rm R} = \mathbf{G}^{\rm r}_{\rm RL}\mathbf{b}_{\rm L}, \tag{86}$$

where we have marked the matrix blocks, M, L, and R explicitly.

We can now deduce transmission probabilities from the general expressions for current in a scattering process as

$$\begin{aligned} T^{\rm SSP}_{{\rm L}\sigma} &= \frac{1}{i}(\mathbf{c}^\dagger_{\rm L}\mathbf{V}_{\rm LM}\mathbf{c}_{\rm M} - \mathbf{c}^\dagger_{\rm M}\mathbf{V}_{\rm ML}\mathbf{c}_{\rm L}), \\ T^{\rm SSP}_{{\rm R}\sigma} &= \frac{1}{i}(\mathbf{c}^\dagger_{\rm M}\mathbf{V}_{\rm MR}\mathbf{c}_{\rm R} - \mathbf{c}^\dagger_{\rm R}\mathbf{V}_{\rm RM}\mathbf{c}_{\rm M}), \end{aligned} \tag{87}$$

where the first equality gives the current from L to M, and the second from M to R.

Using Dyson's equation in the form of Eq. (33), and accounting for the block diagonal nature of the undressed GFs, the SSP vector becomes

$$\begin{aligned} \mathbf{c}_{\rm M} &= \mathbf{G}^{\rm r}_{\rm MM}\mathbf{V}_{\rm ML}\mathbf{g}^{\rm r}_{\rm LL}\mathbf{b}_{\rm L}, \\ \mathbf{c}_{\rm L} &= (\mathbf{g}^{\rm r}_{\rm LL} + \mathbf{g}^{\rm r}_{\rm LL}\mathbf{V}_{\rm LM}\mathbf{G}^{\rm r}_{\rm MM}\mathbf{V}_{\rm ML}\mathbf{g}^{\rm r}_{\rm LL})\mathbf{b}_{\rm L}, \\ \mathbf{c}_{\rm R} &= \mathbf{g}^{\rm r}_{\rm RR}\mathbf{V}_{\rm RM}\mathbf{G}^{\rm r}_{\rm MM}\mathbf{V}_{\rm ML}\mathbf{g}^{\rm r}_{\rm LL}\mathbf{b}_{\rm L}. \end{aligned} \tag{88}$$

If we look first at the transmission in the right-hand lead, substitution of Eqs. (88) into Eq. (87), using the cyclic property of the trace, gives

$$\begin{aligned} T^{\rm SSP}_{{\rm R}\sigma} &= -\frac{1}{i}{\rm tr}\mathbf{G}^{\rm a}_{\rm MM}\mathbf{V}_{\rm MR}\Delta\mathbf{g}_{\rm RR}\mathbf{V}_{\rm RM}{\rm tr}\mathbf{G}^{\rm r}_{\rm MM} \\ &\quad \times \mathbf{V}_{\rm ML}\mathbf{g}^{\rm r}_{\rm LL}\mathbf{b}_{\rm L}\mathbf{b}^\dagger_{\rm L}\mathbf{g}^{\rm a}_{\rm LL}\mathbf{V}_{\rm LM} \\ &= {\rm tr}\mathbf{G}^{\rm a}_{\rm MM}\mathbf{\Gamma}^{\rm R}_{\rm MM}{\rm tr}\mathbf{G}^{\rm r}_{\rm MM} \\ &\quad \times \mathbf{V}_{\rm ML}\mathbf{g}^{\rm r}_{\rm LL}\mathbf{b}_{\rm L}\mathbf{b}^\dagger_{\rm L}\mathbf{g}^{\rm a}_{\rm LL}\mathbf{V}_{\rm LM}. \end{aligned} \tag{89}$$

Comparison with Eq. (58), keeping in mind Eq. (59), implies that

$$\mathbf{V}_{\rm ML}\mathbf{g}^{\rm r}_{\rm LL}\mathbf{b}_{\rm L}\mathbf{b}^\dagger_{\rm L}\mathbf{g}^{\rm r}_{\rm LL}\mathbf{V}_{\rm LM} = \Gamma^{\rm L}_{\rm MM}, \tag{90}$$

is a *sufficient* condition ensuring that the correlated SSP and LB formulae for elastic transmission are identical. From the definition in

Eq. (42),

$$\mathbf{g}^{\mathrm{r}}_{\mathrm{LL}}\mathbf{b}_{\mathrm{L}}\mathbf{b}^{\dagger}_{\mathrm{L}}\mathbf{g}^{\mathrm{a}}_{\mathrm{LL}} = i(\mathbf{g}^{\mathrm{r}}_{\mathrm{LL}} - \mathbf{g}^{\mathrm{a}}_{\mathrm{LL}}), \tag{91}$$

and hence

$$\begin{aligned}\mathbf{b}_{\mathrm{L}}\mathbf{b}^{\dagger}_{\mathrm{L}} &= i(\bar{\mathbf{g}}^{\mathrm{a}}_{\mathrm{LL}})^{-1}(\mathbf{g}^{\mathrm{r}}_{\mathrm{LL}} - \mathbf{g}^{\mathrm{a}}_{\mathrm{LL}})(\bar{\mathbf{g}}^{\mathrm{r}}_{\mathrm{LL}})^{-1} \\ &= i\left((\bar{\mathbf{g}}^{\mathrm{a}}_{\mathrm{LL}})^{-1} - (\bar{\mathbf{g}}^{\mathrm{r}}_{\mathrm{LL}})^{-1}\right).\end{aligned} \tag{92}$$

where $\bar{\mathbf{g}}^{\mathrm{x}}_{\mathrm{LL}}$ is the inverse of the first n_{L} elements of the matrix $\mathbf{g}^{\mathrm{x}}_{\mathrm{LL}}$. We can use Eq. (82) and its complex conjugate to show that

$$i\left((\bar{\mathbf{g}}^{\mathrm{a}}_{\mathrm{LL}})^{-1} - (\bar{\mathbf{g}}^{\mathrm{r}}_{\mathrm{LL}})^{-1}\right) = \begin{pmatrix}\mathbf{0} & \mathbf{0} \\ \mathbf{0} & 2\beta_{\mathrm{L}}\sin q_{\mathrm{L}}\end{pmatrix}. \tag{93}$$

It is now evident that the choice of inhomogeneity term in the SSP equation Eq. (77) is a sufficient condition for

$$T^{\mathrm{SSP}}_{\mathrm{R}\sigma} = T^{\mathrm{LB}}_{\mathrm{L}\sigma} = T^{\mathrm{LB}}_{\mathrm{R}\sigma}, \tag{94}$$

so that the correlated SSP and LB formulae give exactly the same elastic transmission.

To close the circle, we now find the the SSP current in the left lead. Derivation of the L to M current from Eq. (87), $T^{\mathrm{SSP}}_{\mathrm{L}\sigma}$, is a little more involved. Using the same methodology as for the right-hand transmission,

$$\begin{aligned}T^{\mathrm{SSP}}_{\mathrm{L}\sigma} = \frac{1}{i}\mathrm{tr}\boldsymbol{\Gamma}^{\mathrm{L}}_{\mathrm{MM}}\left(\mathbf{G}^{\mathrm{a}}_{\mathrm{MM}}\mathbf{V}_{\mathrm{ML}}\Delta\mathbf{g}_{\mathrm{LL}}\mathbf{V}_{\mathrm{LM}}\mathbf{G}^{\mathrm{r}}_{\mathrm{MM}}\right. \\ \left. - \Delta\mathbf{G}_{\mathrm{MM}}\right),\end{aligned} \tag{95}$$

where we have imposed Eq. (90) once more. We can re-express the $\Delta\mathbf{G}_{\mathrm{MM}}$ term in Eq. (95) using Eq. (50) so that it becomes

$$T^{\mathrm{SSP}}_{\mathrm{L}\sigma} = \mathrm{tr}\mathbf{G}^{\mathrm{r}}_{\mathrm{MM}}\left\{\boldsymbol{\Gamma}^{\mathrm{R}}_{\mathrm{MM}} + i\Delta\mathbf{M}_{\mathrm{MM}}\right\}\mathbf{G}^{\mathrm{a}}_{\mathrm{MM}}\boldsymbol{\Gamma}^{\mathrm{L}}_{\mathrm{MM}}, \tag{96}$$

which apparently contains a non-Landauer term through the correlation self-energy factor. However, as we have seen in section 2.4.2, the non-Landauer term vanishes, and

$$T^{\mathrm{SSP}}_{\mathrm{L}\sigma} = T^{\mathrm{SSP}}_{\mathrm{R}\sigma} = T^{\mathrm{LB}}_{\mathrm{L}\sigma} = T^{\mathrm{LB}}_{\mathrm{R}\sigma}. \tag{97}$$

We conclude that the correlated SSP equation provides a practical route for obtaining correlated expressions for the elastic transmission using modifications of standard quantum chemical procedures.

2.6 Channels for Conduction

The development so far in this section has been for fully general SSP devices in the sense of Figure 1. For the final part of this section, we revert to devices with *simple* connections between molecule and leads as outlined in section 2.1. Such a connection mode maximises the influence of the electronic structure of the molecule on the conduction process.

The solutions to the correlated SSP equations can be obtained by using matrix partitioning. The first row of Eq. (84) can be solved to give $\mathbf{c}_{\mathrm{M}}$ in terms of the lead coefficients as

$$\mathbf{c}_{\mathrm{M}} = \mathbf{g}^{\mathrm{r}}_{\mathrm{MM}}(\mathbf{V}_{\mathrm{ML}}c_{\mathrm{L}} + \mathbf{V}_{\mathrm{MR}}c_{\mathrm{R}}). \tag{98}$$

The Lehmann spectral expansion[27] of the advanced GF can be written as

$$\begin{aligned}(\mathbf{g}^{\mathrm{r}}_{\mathrm{MM}})_{\mathrm{pq}} = \sum_{\lambda}\frac{f_{\lambda\mathrm{p}}f^{*}_{\lambda\mathrm{q}}}{\mathcal{E}^{\mathrm{r}} - E^{N}_{0} + E^{N-1}_{\lambda}} \\ + \sum_{\lambda}\frac{f_{\lambda\mathrm{q}}f^{*}_{\lambda\mathrm{p}}}{\mathcal{E}^{\mathrm{r}} + E^{N}_{0} - E^{N+1}_{\lambda}}.\end{aligned} \tag{99}$$

The quantities defined in the numerators in Eq. (99) are coefficients of the *Dyson orbitals* (DOs), expanded in terms of a basis of HF molecular spin-orbitals $\{\phi_{\mathrm{p}}\}$. The DO coefficients are

$$\begin{aligned}f_{\lambda\mathrm{p}} &= \langle\Psi^{N-1}_{\lambda}|a^{\dagger}_{\mathrm{p}}|\Psi^{N}_{0}\rangle \text{ ionisation poles,} \\ f_{\lambda\mathrm{p}} &= \langle\Psi^{N}_{0}|a^{\dagger}_{\mathrm{p}}|\Psi^{N+1}_{\lambda}\rangle \text{ attachment poles.}\end{aligned} \tag{100}$$

The first term in the Lehmann representation is a sum over $(N-1)$-electron states (corresponding to hole conduction), whilst the second is over $(N+1)$-electron states (corresponding to particle conduction). The poles of the one-electron GF give, in principle, the exact ionisation and attachment energies.

The equations for the leads, after elimination of $\mathbf{c}_{\mathrm{M}}$ by substituting Eq. (98) into the SSP

equations for $c_{\rm L}$ and $c_{\rm R}$, give

$$\begin{pmatrix} a & b \\ b^* & c \end{pmatrix} \begin{pmatrix} c_{\rm L} \\ c_{\rm R} \end{pmatrix} = \begin{pmatrix} -iN_{\rm L} \\ 0 \end{pmatrix}, \tag{101}$$

in which

$$\begin{aligned} a &= \beta_{\rm L} e^{-iq_{\rm L}} - \mathbf{V}_{\rm ML}\mathbf{g}^{\rm r}_{\rm MM}\mathbf{V}_{\rm ML} \\ &= \beta_{\rm L} e^{-iq_{\rm L}} - \beta^2_{\overline{\rm L}\,{\rm L}} \sum_\lambda \frac{|f_{\overline{\rm L}\lambda}|^2}{E-\xi_\lambda}, \\ b &= -\mathbf{V}_{\rm ML}\mathbf{g}^{\rm r}_{\rm MM}\mathbf{V}_{\rm MR} \\ &= -\beta_{\overline{\rm L}\,{\rm L}}\beta_{\overline{\rm R}\,{\rm R}} \sum_\lambda \frac{f_{\overline{\rm L}\lambda} f^*_{\overline{\rm R}\lambda}}{E-\xi_\lambda}, \\ c &= \beta_{\rm R} e^{-iq_{\rm R}} - \mathbf{V}_{\rm MR}\mathbf{g}^{\rm r}_{\rm MM}\mathbf{V}_{\rm MR} \\ &= \beta_{\rm R} e^{-iq_{\rm R}} - \beta^2_{\overline{\rm L}\,{\rm L}} \sum_\lambda \frac{|f_{\overline{\rm R}\lambda}|^2}{E-\xi_\lambda}. \end{aligned} \tag{102}$$

Here, we have used Eq. (99) to write the GFs in terms of poles and Dyson orbital amplitudes. We can immediately recognise that

$$\begin{aligned} \hat{t} &= \sum_\lambda \frac{|f_{\overline{\rm L}\lambda}|^2}{E-\xi_\lambda}, \hat{u} = \sum_\lambda \frac{|f_{\overline{\rm R}\lambda}|^2}{E-\xi_\lambda}, \\ \hat{j} &= \sum_\lambda \frac{f_{\overline{\rm L}\lambda} f^*_{\overline{\rm R}\lambda}}{E-\xi_\lambda}, \end{aligned} \tag{103}$$

are the correlated analogues of the hatted structural polynomials (SPs) defined in Eq. (17). Here, the Hückel MO coefficients have been replaced by Dyson orbital coefficients, and the Hückel orbital energies by (undressed) GF pole energies.

Simple algebra leads directly to an expression for the transmission that has exactly the form of Eq. (15) but now with correlated definitions to replace those of Eq. (17). The correlated SPs satisfy the same interlacing theorems as their Hückel theory counterparts.[102] We can, therefore, take over all the machinery derived in the Hückel case[73] for the interpretation of conduction in terms of internal conduction channels and selection rules.

Degenerate poles in Eq. (99) constitute a 'Dyson shell'. We can use the correlated SSP equations to derive an expression[73] for the current through a shell Λ as

$$J_{{\rm L}\to\Lambda,\sigma} = \mathcal{B} \sum_{\lambda\in\Lambda} \frac{f_{\overline{\rm L}\lambda} f^*_{\overline{\rm R}\lambda}}{E-\xi_\lambda} \frac{\hat{j}}{|\hat{D}|^2}, \tag{104}$$

where $\hat{D} = D/s$, and $\mathcal{B}$ is given by Eq. (11). In common with any orbital-based partition, individual shell currents may be negative, or may exceed unity for parts of the energy range.[73] However, the shell currents satisfy the sum rule, in that they add up to the total transmission. Dyson shells emerge naturally using the correlated SSP method as a description of internal conduction channels.

The classification of internal channels as *inert* or *active*[73] also applies to the correlated SSP method. Active shells conduct, and give rise to specific maxima in the transmission function. Inert shells do not conduct at any energy and have no influence on the shape of the transmission function. The inert/active distinction can be used to give a considerable saving of computational effort in determining the shell currents and the transmission function.

The existence of hatted SPs for the correlated SSP method enables the conduction properties of a two-lead device at GF pole energies to be classified in terms of 11 cases for distinct contact atoms (3 cases for ipso devices with identical contact atoms, $\overline{\rm L} = \overline{\rm R}$). The cases can be determined using the number of repeated roots in the SPs.[76] Conduction may occur at the poles corresponding to inert shells, but then occurs only through the other active shells. DO-based SPs retain the interlacing properties of their uncorrelated counterparts, even though they can no longer be associated with specific unweighted graphs.

One small technical detail is that we have not defined the s polynomial for the correlated SSP equations. The appropriate definition is through GF ionisation and attachment, by analogy with Hückel theory as:

$$s = \prod_\lambda (E-\xi_\lambda), \tag{105}$$

where the product ranges over attachment poles ($\xi_\lambda = E^{N+1}_\lambda - E^N_0$), and ionisation poles ($\xi_\lambda =$

$E_0^N - E_\lambda^{N-1}$). With this choice for s, the correlated versions of hatless polynomials$t$, u, j, and v can all be recovered.

3 Calculations

In this section we present some practical applications of the SSP technique for solving the correlated LB equations. We choose a tight-binding (Hückel) *molecular* Hamiltonian to which we add two kinds of electron interaction term. The first is the Hubbard interaction[81] which comprises single-centre two-electron integrals, each of which is set equal to a parameter, U. The second term includes two-centre two-electron integrals[82,83] set to a parameter, W. We restrict these terms to atoms that are directly π-bonded. We refer to this as the *edge-PPP* (ePPP) method, since directly bonded atoms are represented by graph edges in graph theory. ePPP is a simple extension to the one-electron tight-binding method with only two extra parameters. The Hamiltonian is

$$H_{\mathrm{ePPP}} = H_{\mathrm{Hück}} + U\beta_{\mathrm{M}} \sum_{\mathrm{p}} n_{\mathrm{p}\alpha} n_{\mathrm{p}\beta} + W\beta_{\mathrm{M}} \sum_{\mathrm{p}\sim\mathrm{q}} n_{\mathrm{p}} n_{\mathrm{q}}, \qquad (106)$$

where the occupation-number operators are

$$n_{\mathrm{p}\sigma} = a^\dagger_{\mathrm{p}\sigma} a_{\mathrm{p}\sigma}, \quad n_{\mathrm{p}} = n_{\mathrm{p}\alpha} + n_{\mathrm{p}\beta}. \qquad (107)$$

We have arbitrarily used values of $U = -\beta_{\mathrm{M}}$, and $W = -\beta_{\mathrm{M}}/2$ in all calculations. Electron repulsion in the HF and correlated calculations causes the GF poles to shift to higher energies. Since the lead Hamiltonians are constructed from one-electron Hamiltonians (i.e. not having any electron repulsion terms included) it was felt appropriate to re-centre the molecular GF spectra so that the Fermi level of the molecule was at zero in units of β_{M}.

All calculations were carried out with our own software using the Maple 2019 computer algebra program.[103] The transmission was calculated for two-lead unbiassed symmetric devices, i.e. with lead parameters $\alpha_{\mathrm{L}} = \alpha_{\mathrm{R}} = 0$, with $\beta_{\mathrm{L}} = \beta_{\mathrm{R}} = 3\beta_{\mathrm{M}}$, and $\beta_{\mathrm{M}} = -1$.

We used three levels of approximation, the lowest being the Hückel (tight-binding) approximation, and the second being HF with a closed-shell wavefunction. Finally, we computed the correlated GFs at second-order (GF2) using the HF ground-state function as a reference. The GF2 equations for the molecule were constructed and solved using the superoperator technique.[104] The operator basis for the GF2 superoperator matrix contains the single operators $\{a_{\mathrm{p}\alpha}\}$ that dominate the Koopmans configurations,[105,106] and hole-hole-particle and particle-particle-hole operators (the h_3-operators) for describing 'shake' configurations. GF2 overestimates the correlation corrections to Koopmans ionization and attachment energies, and shake states are poorly described, but it does give a lowest order account of the effects of electron correlation and is computationally tractable. A detailed discussion of the accuracy of GF calculations of ionisation energies in molecules is given by Ortiz et al.[107]

The dimension of the GF2 superoperator matrix, after accounting for spin, is $(n+m)(nm+1)$, where n is the number of occupied, and m is the number of virtual orbitals in the HF basis. Diagonalization of the superoperator Hamiltonian matrix gives the GF2 pole energies and the Dyson orbitals used to construct the SSP secular equations, which were then solved at each particle/hole energy, E.

Transmission curves were obtained by taking 1000 evenly spaced points across the band. Three extra energy points were inserted at each peak maximum and half-height point, to ensure that all peaks (including shake peaks) were sampled. Peak widths and half-height points were estimated using a perturbation expansion for the complex-valued dressed GF poles.

Results of calculations are shown for butadiene (Fig. 3), benzene (Fig. 4) and pentalene (Fig. 5). The Hückel results are in part a) of each figure, whilst parts b) and c) contain HF and GF2 results, respectively. The undressed molecular GF pole energies are marked with vertical lines, coloured red for ionisation (hole conduction) and blue for attachment (particle conduction). Pole lines are solid for Koopmans,

and dotted for shake poles. Shell currents are displayed in solid colour only for the Koopmans conduction channels. All energies are in units of β_{M}.

3.1 Butadiene

The butadiene device has leads attached to separate terminal atoms. All channels are active in each of the calculations. The total transmission and the four individual MO currents at the Hückel level (see Fig. 3a) show four maxima in the transmission, one near each Hückel eigenvalue. Each maximum is dominated by a single shell current that has zero transmission at other pole energies. Transmission is symmetric about $E = 0$ because of the bipartite nature of the molecular graph.[108] The poles of $\mathbf{g}_{\mathrm{MM}}^{\mathrm{Hück}}$ are the Hückel eigenvalues, at ± 1.6180 and ± 0.6180, and the energy splitting between hole states is the same as between particle states. The dressing of the GF arising from the molecule lead-interaction pushes its poles into the complex plane. Thus, the poles of $\mathbf{G}_{\mathrm{MM}}^{\mathrm{Hück}}$ are at $\pm 1.6343 \pm i0.0950$ and $\pm 0.6343 \pm i0.2532$. The poles in $\mathbf{G}_{\mathrm{MM}}^{\mathrm{r}}$ are the zeroes of the denominator $D(E)$ in the formula in Eq. (10), and their conjugates arise from the complex conjugate GF, $\mathbf{G}_{\mathrm{MM}}^{\mathrm{a}}$ (i.e. from $D(E)^*$). These eight complex poles are responsible for the four peaks shown in the figure. The imaginary components of these resonances are related to their lifetimes.[109] We observe that the outermost two resonances have lifetimes longer by a factor of almost three times the inner.

The HF calculations (see Fig. 3b) used a four-electron closed-shell ground state with two doubly-occupied MOs, so the undressed GF has again four poles, one for each MO. The poles of the HF GF are at 0.6094, -0.3184, -1.9334, and -3.2038. The transmission is not symmetric about any particular energy in the HF case; the splitting between the hole states is 0.928, whilst that between particle states is 1.270.

GF2 (see Fig. 3c) uses the same closed-shell ground state, and gives 20 non-degenerate poles, all lying within the band ($-6 \leq E \leq 6$) and giving active conduction channels. The positions and widths of the Koopmans poles are

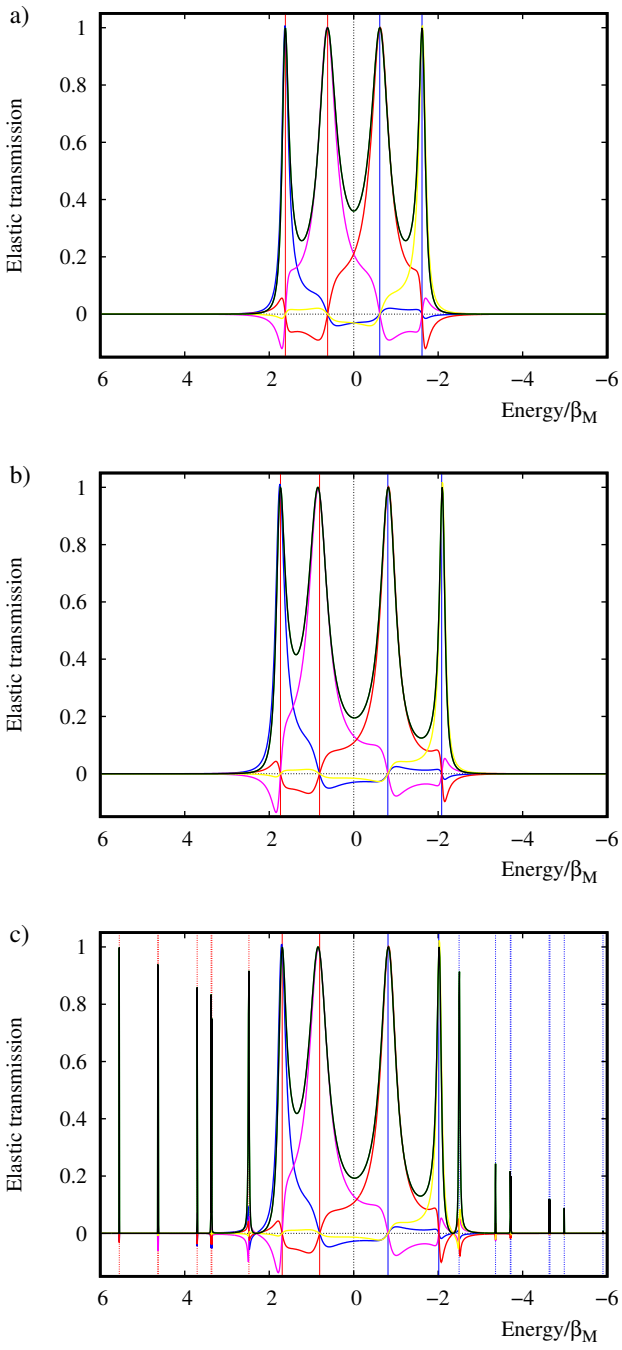

Figure 3: Total transmission (black curves) and Koopmans shell currents (coloured) for end-connected butadiene calculated using a) Hückel, b) HF, and c) GF2 approximations. Vertical lines mark Koopmans (solid)/shake (dotted) poles of the undressed molecular GF; ionisation poles are in red, attachment in blue. Units, Hubbard parameters and centering of the transmission spectrum are described in the text.

similar to those in the HF calculation. The ionisation poles, have DO norms of 0.9367 and 0.9866. The attachment poles have norms of 0.9884 and 0.8674. Departure of the DO norm from unity is a measure of how strongly Koopmans configurations interact with their shake counterparts. The shake poles all have low DO norms, the largest, 0.1252, being from pole 13 at $E = -2.4951$, which is energetically closest to the rightmost Koopmans particle peak. The shifts exhibited by the peaks in T_σ^{LB} are largest in the centre of the band and decrease towards the edges. The same is true of peak widths.

3.2 Benzene

In Hückel theory (see Fig. 4a) the eigenvalues of benzene are 2, 1, -1, and -2, with eigenvector symmetries a_{2u}, e_{1g}, e_{2u}, and b_{2g}, respectively, corresponding to the D_{6h} point group. We present results for the ortho-connected device because in this case the doubly-degenerate shells, e_{1g} and e_{2u}, are split by the lead-molecule interaction, the device having *lower* symmetry than the molecule. The complex *dressed* poles are at energies $\pm 1.0027 \pm 0.0569i$ and $\pm 1.0452 \pm 0.1658i$. These shells are active and produce characteristic double-peak structures around $T_\sigma^{\mathrm{LB}} = 0$ at the Koopmans orbital energy. The meta-device has the same symmetry, but the para- and ipso-devices possess the full molecular symmetry. In these cases the dressed poles remain doubly-degenerate. The non-degenerate levels, a_{2u}, and b_{2g} are also active, each producing a maximum in the spectrum corresponding to the dressed poles at $\pm 2.0199 \pm 0.1198i$.

The HF calculations (see Fig. 4b) use a six-electron closed-shell ground state. The MOs are determined by point group symmetry and are identical to their Hückel counterparts. The eigenvalues, in units of β_{M}, are $2+U/2+4W/3$, $1+U/2+5W/3$, $1+U/2+7W/3$, $-2+U/2+8W/3$, in the order a_{2u}, e_{1g}, e_{2u}, and b_{2g}. As before, we have re-centred the spectrum to allow for the shift to higher values. Peak shapes and splittings differ slightly from the Hückel results.

GF2 (see Fig. 4c) has a superoperator Hamiltonian matrix of dimension 60. The 60

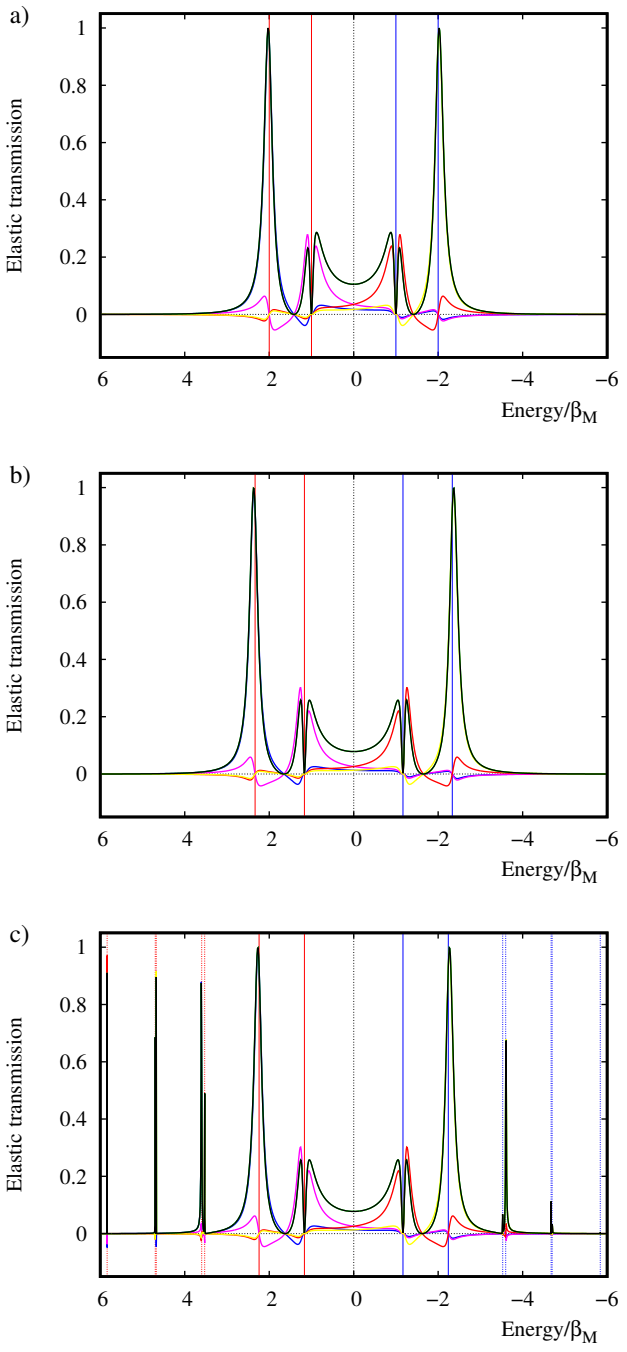

Figure 4: Total transmission (black curves) and Koopmans shell currents (coloured) for ortho-connected benzene calculated using a) Hückel, b) HF, and c) GF2 approximations. Parameters and conventions as in Figure 3.

poles comprise 30 ionisations and 30 attachments. There are many highly degenerate shells, viz. two 9-fold, 5-fold, and 4-fold, and eight 2-fold degenerate shells. The remainder are singly degenerate. Fourteen shells are active, and the rest are inert. The two doubly degenerate shells corresponding to the e_{1g} and e_{2u} Koopmans primary poles produce the double peak structures seen in the Hückel and HF calculations. All double degenerate shells in the spectrum share this property, although it cannot be seen in the figure because of the narrow widths of the shake lines.

The high degeneracy of many of the shells arises because the h_3 basis operator block of the superoperator matrix is *diagonal* and contains only orbital energies. Since there are two doubly-degenerate MO shells at the HF level, there are many degenerate combinations of triple indices. In a higher-order 'non-diagonal' GF approximations,[107,110] two-electron interactions would remove this 'accidental' degeneracy, leaving only the degeneracy coming from point group symmetry.

3.3 Pentalene

At equilibrium the physical pentalene molecule is distorted, with C_{2h} symmetry, but our calculations retain the D_{2h} symmetry of the unweighted graph. We also choose a 'para' device with connections to antipodal vertices in the mirror plane that bisects the ring-fused bond. The molecule is also a non-alternant, so the Hückel transmission shown in Fig. 5a is not symmetric about $E = 0$. With the molecule placed in the xy-plane, Hückel MOs 1, 4 and 7 have b_{1u}, 2 and 6 have b_{2g}, 3 and 8 have b_{3g}, and MO 5 has a_u symmetry. The a_u and b_{3g} orbitals are inert because they are antisymmetric with respect to the mirror plane passing through the contact atoms. Hence, MOs 3, 5 and 8 are inert, and the remaining five MOs are active. This leads to five complex conjugate pairs of dressed poles at $2.3577 \pm 0.0496i$, $1.4463 \pm 0.1715i$, $0.4814 \pm 0.1818i$, $-1.4463 \pm 0.1715i$, and $-1.8391 \pm 0.1113i$. Note that the inert orbital eigenvalues are shown, although there are no corresponding transmission peaks.

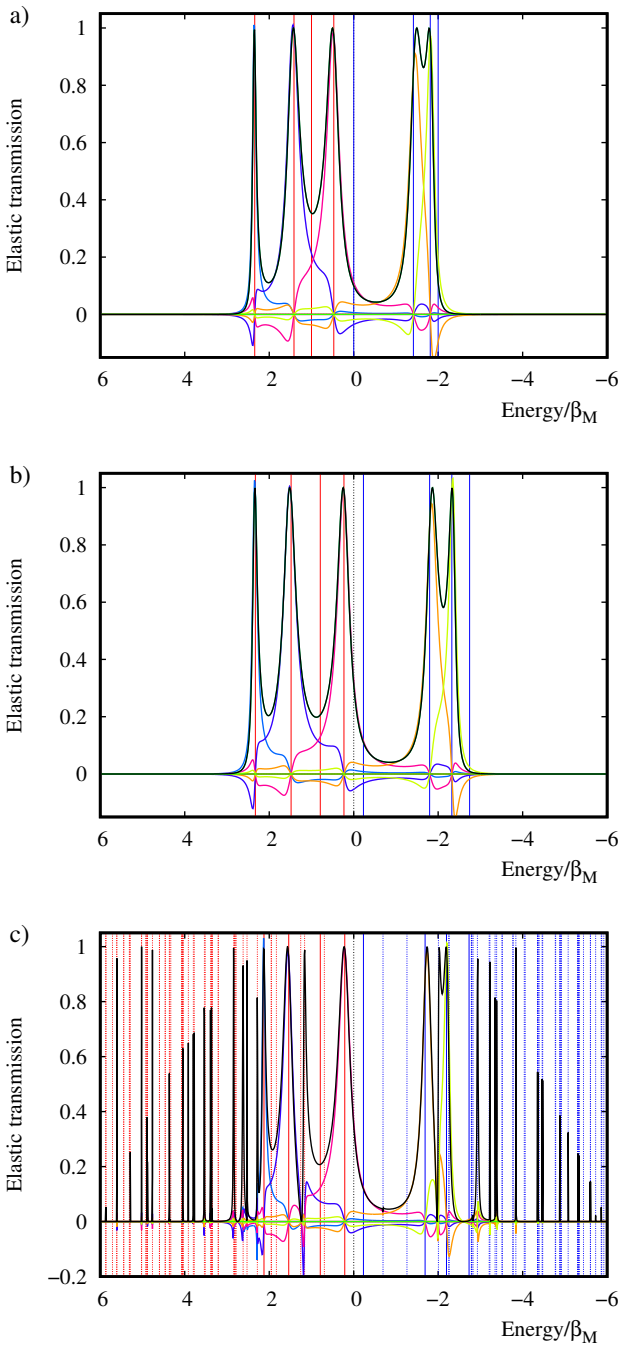

Figure 5: Total transmission (black curves) and Koopmans shell currents (coloured) for symmetrically-connected pentalene calculated using a) Hückel, b) HF, and c) GF2 approximations. Parameters and conventions as in Figure 3.

The HF transmission calculation, (see Fig. 5b) effected using a $1b_{1u}^2 1b_{2g}^2 1b_{3g}^2 2b_{1u}^2$ closed-shell ground state, has exactly the same symmetry analysis. The re-centred transmission graph looks very similar to the Hückel graph, except that again peak heights, splittings and widths are slightly different.

GF2 calculations (see Fig. 5c) were carried out with the same four-electron ground state. There are 128 triple operators in the GF2 basis. Each can easily be classified in terms of the D_{2h} irreducible representations since the group is abelian and the HFMOs are symmetry adapted. Out of a total of 136 operators, only 67 lead to active shells. Pentalene is expected to be typical of larger organic molecules in that it has a plethora of shake peaks. The innermost of these interact strongly with the nearby Koopmans feature, leading to a more complex interpretation of the transmission curve.

4 Discussion

Our aim in this paper was to adapt an existing 'wavefunction' approach to ballistic conduction (the SSP model) to allow for molecular correlation, retaining interpretability as far as possible. The main requirement was that the new approach should produce results exactly equivalent to those from the MW formulation at each given level of molecular-electronic structure theory. This aim has been realised for all rungs on the ladder of electronic-structure approximations from Hückel tight-binding through self-consistent field, to GF treatments of electron correlation.

4.1 Connecting MW and SSP

The first step in this programme was to separate the Landauer and non-Landauer contributions to the MW formula and show that the latter vanishes in the absence of electron-phonon interactions. An extended SSP Ansatz yielding the elastic correlated LB transmission function for a two-lead device was then proposed and verified. As the SSP model gives an explicit device wavefunction, it follows that in the new approach the conduction eigenchannels, which correspond to molecular orbitals (shells) in tight-binding and SCF implementations, have their natural extension in channels based on Dyson orbitals (shells). These channels obey selection rules,[73] albeit based on modified definitions of structural polynomials, and have clear links to ionisation/attachment processes and shake states of the correlated molecular system. The correlated LB formula extracted from the MW formula[19] is symmetric in terms of scattering rate matrices, $\Gamma^{\mathrm{X}}_{\mathrm{MM}}$, between the molecule and the individual leads. The strength and direction of current are dependent on the differences in chemical potential.

Within the SSP model, a device is modelled as a central molecule connected to semi-infinite leads. Leads and their connections to the molecule are described by a one-electron tight-binding (Hückel) Hamiltonian. The molecular Hamiltonian may include one- and two-electron interactions. The molecular part of the problem may therefore be treated with empirical, semi-empirical, or ab initio methods, with or without inclusion of correlation. ab initio calculations with SSP have been undertaken by Fias[56] et al. using the DFT method to describe the molecule.

In contrast to our previous work,[53,73] our zeroth-order starting approximation here is the fully correlated molecule, with internal electron-electron interactions treated to arbitrary accuracy, so the embedding self-energies that we use depend on the leads and the lead-molecule interaction only.

4.2 Consequences for Interpretation

In the second step, we establish the consistency of the correlated LB formula with respect to a proposed modification of the SSP equations. In contrast to NEGF methods, the transmission in the SSP approach is determined by boundary conditions on a device wavefunction. The conceptual advantages of this wavefunction-based method lie in the *chemical* interpretability of the internal molecular channels for conduction.

These channels are determined by the attached and ionised states appearing in the Lehmann representation of the equilibrium molecular GF. The properties of these channels are defined in terms of the characteristics of the Dyson orbitals associated with each of the GF poles. The sets of orbitals and poles define spectral expansions of structural polynomials, which in turn generate selection rules. The relevant formal properties of the polynomials are retained *regardless of the level of theory*, from Hückel through to sophisticated GF formalisms.

Channel analysis of this kind gives a ready interpretation of the transmission curves that we have calculated. These have peaks arising from both Koopmans and shake GF poles. The Koopmans poles produce broad peaks. The poles of the dressed GF corresponding to each of these Koopmans peaks have larger imaginary parts than their shake counterparts. Dyson orbitals offer a means by which ionisation and attachment sectors can be identified from the structure of the DO coefficients for a given peak of the transmission spectrum, corresponding to the red and blue regions in the figures. Each peak may be classified as being due to hole or to particle conduction.

4.3 Relevance to Pauli Blockade

Pauli blockade has been observed in quantum dots in situations where electrons can jump between dots already containing electrons. Electron transport through a generic two-site system has been reported,[78] with one electron trapped permanently on the second site. For reverse bias, a transport channel through two-electron singlet states is always available. In the reported experiment, for a sufficiently large forward bias, a triplet state with an electron on each site is sooner or later occupied and further electron transport is blocked due to Pauli exclusion. The device acts as a current rectifier. A similar case is reported by Kodera et al.[79]

To describe such cases, one could modify the tight-binding SSP method[74,96] so that a device wavefunction is constructed from all electron configurations with a fixed molecular core topped by an orbital relevant to the scattered electron. Such an approach would be different from the GF methods described in this paper. One could adopt a CI approach based upon an N-electron molecular HF ground state configuration, in which configurations with a single *extra* electron were used to describe the scattered electron. We have used this approach (without two-electron interactions) in our previous work.[74] Of necessity, this (CI) wavefunction represents electron transmission through virtual molecular orbitals *only* and results in a truncated transmission spectrum which is suppressed at energies corresponding to occupied orbitals. This CI *Ansatz* is appropriate to experimental situations in which the number of electrons in the device is well specified, and where bias eliminates hole-conduction terms. In contrast, the present GF approach includes both particle- and hole-conduction via virtual and occupied manifolds and restores the transmission function at low energy. An alternative CI-based SSP method for separate treatment of hole-conduction could be envisaged using only $(N-1)$-electron molecular configuration functions. Finally, we note that efficient implementation of the correlated LB equation is possible because the transmission depends only on GFs, which can be computed using minor changes to pre-existing codes. The efficiency comes from the reformulation of the correlated LB equation is terms of the SSP model. The algorithm is separated into two parts. First we solve for the molecular GF equations for those pole energies and DOs that are important for the conduction process. These data feed into the SSP equations to be solved for a series of incoming particle/hole energies. The transmission calculations, therefore, are not affected by the degree of sophistication used to describe the molecular GF.

4.4 Consequences for calculations

Finally, the separation of the MW formula into Landauer and non-Landauer terms may have some useful consequences for alternative methods for calculation of transmission. The correlation self-energy has the correct functional form in the present approach, where electron-

electron interaction within the molecule is taken fully into account before coupling to the leads. This is the key to the elimination of non-symmetric terms in the MW formula and ensures conservation of current.

Conservation of current in GF calculations of MED transmission is usually imposed by requiring that the self-energy be a derivative of the well-known $\Phi(G)$ functional.[27] Hence, the self-energy depends implicitly upon the dressed GF for the whole device. The GF, therefore, needs to be determined self-consistently. A commonly used method is the GW approach.[37,43,44] The present work shows that current conservation can be achieved without self-consistency. It should be said, however, that relinquishing self-consistency involves the algebraic diagrammatic construction[88] of the self-energy, which is also computationally expensive, especially if taken beyond GF2.

In this paper we have restricted ourselves to the calculation of the transmission, T, at zero bias. The calculation of I-V curves requires repeated calculations of T for different values of lead bias potential. In our approach, the correlation self-energy is unaffected by the lead bias, because the *undressed* molecular GF, $\mathbf{g}_{\mathrm{MM}}$, does not experience *any* effects from the leads, so the poles of the self-energy do not shift. The GW method, on the other hand, includes diagrammatic contributions from the contact potential, $\mathbf{V}$, *inside* correlation self-energy terms as required for self-consistency.

5 Conclusion

The Meijer-Wingreen formula, the starting point of our work, gives an exact expression for the current through a molecular device described using one-electron leads and lead-molecule interaction, but with a Born-Oppenheimer Hamiltonian for the molecule. The leads and the molecule, in the absence of lead-molecule interactions are in separate equilibrium states. This implies that corresponding (lesser) GFs satisfy exactly the fluctuation-dissipation theorem. This allows us to use standard Dyson and Keldysh equations of NEGF theory to show that one term in the expression for current derived from the Meir-Wingreen formula is exactly zero when electron-phonon interactions are neglected. We have shown that the remaining elastic-scattering term is a Landauer-Büttiker expression that is symmetric in the leads and includes the effects of molecular electron correlation, in principle, exactly.

The correlated expression for transmission can be computed using an extension of the SSP model. This mode of calculation provides access to internal conduction channels associated with the SSP wavefunction, and a quasiparticle interpretation of conduction with lifetimes connected to the imaginary parts of the pole energies of the dressed GF. The conduction channels can be analysed in terms of the same small set of conduction cases derived previously for the tight-binding approximation.[76] The molecular part of the calculations may be conducted using ab initio or semi-empirical methods. Some illustrative calculations with a simple model Hamiltonian show the qualitative effects of inclusion of intramolecular electron interaction on elastic transmission.

Acknowledgement The authors thank Stijn Fias and Thijs Stuyver for discussions on ab initio calculations of conduction through molecules, and a rightly persistent referee for a stimulating debate on the nature of elastic and inelastic contributions to transmission. This research was not funded by any public or commercial agencies.

References

(1) Aviram, A.; Ratner, M. A. Molecular rectifiers. *Chem. Phys. Lett.* **1974**, *29*, 277–283.

(2) Nature Nanotechnology, *Molecular Electronics Focus Issue*; Springer Nature, 2013; Vol. 8; pp 377–467.

(3) Nichols, R. J.; Higgins, S. J. Single-Molecule Electronics: Chemical and Analytical Perspectives. *Ann. Rev. Anal. Chem.* **2015**, *8*, 389–417.

(4) Xiang, D.; Wang, X.; Jia, C.; Lee, T.; Guo, X. Molecular-Scale Electronics: From Concept to Function. *Chem. Rev.* **2016**, *116*, 4318–4440.

(5) Mathew, P. T.; Fang, F. Advances in Molecular Electronics: A Brief Review. *Engineering* **2018**, *4*, 760 – 771.

(6) Xin, N.; Guan, J.; Zhou, C.; Chen, X.; Gu, C.; Li, Y.; Ratner, M. A.; Nitzan, A.; Stoddart, J. F.; Guo, X. Concepts in the design and engineering of single-molecule electronic devices. *Nature Reviews Physics* **2019**, *1*, 211–230.

(7) Chen, B.; Xu, K. Single Molecule-Based Electronic Devices: A Review. *Nano* **2019**, *14*, 1930007.

(8) Cohen, G.; Galperin, M. Green's function methods for single molecule junctions. *The Journal of Chemical Physics* **2020**, *152*, 090901.

(9) Landauer, R. Spatial variation of currents and fields due to localized scatterers in metallic conduction. *IBM J. Res. Dev.* **1957**, *1*, 223–231.

(10) Imry, Y. In *Directions in Condensed Matter Physics*; Grinstein, G., Mazenko, G., Eds.; World Scientific Publishers, 1986; p 101.

(11) Hall, L. E.; Reimers, J. R.; Hush, N. S.; Silverbrook, K. Formalism, analytical model, and a priori Greens-function-based calculations of the current-voltage characteristics of molecular wires. *J. Chem. Phys.* **2000**, *112*, 1510–1521.

(12) Cuevas, J. C.; Scheer, E. *Molecular Electronics: An Introduction to Theory and Experiment*; World Scientific: Singapore, 2010.

(13) Mujica, V.; Kemp, M.; Ratner, M. A. Electron conduction in molecular wires. I. A scattering formalism. *J. Chem. Phys.* **1994**, *101*, 6849–6855.

(14) Mujica, V.; Kemp, M.; Ratner, M. A. Electron conduction in molecular wires. II. Application to scanning tunnelling microscopy. *J. Chem. Phys.* **1994**, *101*, 6856–6864.

(15) Mujica, V.; Kemp, M.; Roitberg, A.; Ratner, M. Current-voltage characteristics of molecular wires: eigenvalue staircase, Coulomb blockade, and rectification. *J. Chem. Phys.* **1996**, *104*, 7296–7305.

(16) Datta, S. *Quantum Transport: Atom to Transistor*; Cambridge University Press: Cambridge, UK, 2013.

(17) Tian, W.; Datta, S.; Hong, S.; Reifenberger, R.; Henderson, J. I.; Kubiak, C. P. Conductance spectra of molecular wires. *J. Chem. Phys.* **1998**, *109*, 2874–2882.

(18) Caroli, C.; Combescot, R.; Noziéres, P.; Saint-James, D. A direct calculation of the tunneling current: IV. Electron-phonon effects. *J. Phys. C. Solid State Phys.* **1972**, *5*, 21–42.

(19) Meir, Y.; Wingreen, N. S. Landauer formula for the current through an interacting electron region. *Phys. Rev. Lett.* **1992**, *68*, 2512–2515.

(20) Kadanoff, L. P.; Baym, G. *Quantum Statistical Mechanics*; W.A. Benjamin, 1962.

(21) Baym, G. Self-consistent approximations in many-body systems. *Phys. Rev.* **1962**, *171*, 1391–1401.

(22) Keldysh, L. V. Diagram technique for non-equilibrium processes. *Zh. Eksp. Teor. Fiz.* **1964**, *47*, 1515.

(23) Keldysh, L. V. Diagram technique for non-equilibrium processes. *Sov. Phys. JETP* **1965**, *20*, 1018.

(24) Taylor, J.; Guo, H.; Wang, J. Ab initio modeling of open systems: Charge transfer, electron conduction, and molecular

switching of a C_{60} device. *Phys. Rev. B* **2001**, *63*, 121104.

(25) Taylor, J.; Guo, H.; Wang, J. Ab initio modelling of quantum transport properties of molecular electronic devices. *Phys. Rev. B* **2001**, *63*, 245407.

(26) Brandbyge, M.; Mozos, J.-L.; Ordejón, P.; Taylor, J.; Stokbro, K. Density-functional method for nonequilibrium electron transport. *Phys. Rev. B* **2002**, *65*, 165401.

(27) Stefanucci, G.; van Leeuwen, R. *Nonequilibrium Many-Body Theory of Quantum Systems*; Cambridge University Press: Cambridge, UK, 2013.

(28) Chong, D. P.; Gritsenko, O. V.; Baerends, E. J. Interpretation of the Kohn-Sham orbital energies as approximate vertical ionization potentials. *J. Chem.Phys.* **2002**, *116*, 1760–1772.

(29) Baerends, E. J.; Gritsenko, O. V.; van Meer, R. The Kohn-Sham gap, the fundamental gap and the optical gap: the physical meaning of occupied and virtual Kohn-Sham orbital energies. *Phys. Chem. Chem. Phys.* **2013**, *15*, 16408–16425.

(30) Perdew, J. P.; Parr, R. G.; Levy, M.; Balduz, J. L. Density-Functional Theory for Fractional Particle Number: Derivative Discontinuities of the Energy. *Phys. Rev. Lett.* **1982**, *49*, 1691–1694.

(31) Perdew, J. P.; Levy, M. Physical Content of the Exact Kohn-Sham Orbital Energies: Band Gaps and Derivative Discontinuities. *Phys. Rev. Lett.* **1983**, *51*, 1884–1887.

(32) Sham, L. J.; Schlüter, M. Density-Functional Theory of the Energy Gap. *Phys. Rev. Lett.* **1983**, *51*, 1888–1891.

(33) Kümmel, S.; Kronik, L. Orbital-dependent density functionals: Theory and applications. *Rev. Mod. Phys.* **2008**, *80*, 3–60.

(34) Kronik, L.; Stein, T.; Refaely-Abramson, S.; Baer, R. Excitation Gaps of Finite-Sized Systems from Optimally Tuned Range-Separated Hybrid Functionals. *J. Chem. Theory Comput.* **2012**, *8*, 1515–1531.

(35) Zhou, Y.; Ernzerhof, M. Open-system Kohn-Sham density functional theory. *J. Chem. Phys.* **2012**, *136*, 094105.

(36) Delaney, P.; Greer, J. C. Correlated Electron Transport in Molecular Electronics. *Phys. Rev. Lett.* **2004**, *93*, 036805.

(37) Thygesen, K. S.; Rubrio, A. Conserving GW scheme for nonequilibrium transport in molecular contacts. *Phys. Rev. B* **2008**, *77*, 115333.

(38) Niu, C.; Liu, L.; Lin, T. Coherent transport through a coupled-quantum-dot system with strong intradot interaction. *Phys. Rev. B* **1995**, *51*, 5130–5137.

(39) Lamba, S.; Joshi, S. K. Transport through a coupled quantum dot system: Role of interdot interactions. *Phys. Rev. B* **2000**, *62*, 1580–1583.

(40) Bułka, B. R.; Kostyrko, T. Electronic correlations in coherent transport through a two quantum dot system. *Phys. Rev. B* **2004**, *70*, 205333.

(41) Chang, Y.-C.; Kuo, D. M.-T. Theory of charge transport in a quantum dot tunnel junction with multiple energy levels. *Phys. Rev. B* **2008**, *77*, 245412.

(42) Hedin, L. New Method for Calculating the One-Particle Green's Function with Application to the Electron-Gas Problem. *Phys. Rev.* **1965**, *139*, A796–A823.

(43) Darancet, P.; Ferretti, A.; Mayou, D.; Olevano, V. Ab initio *GW* electron-electron interaction effects in quantum transport. *Phys. Rev. B* **2007**, *75*, 075102.

(44) Moldoveanu, V.; Tanatar, B. Coulomb effects in open quantum dots within

the random-phase approximation. *Phys. Rev. B* **2008**, *77*, 195302.

(45) Jin, C.; Strange, M.; Markussen, T.; Solomon, G. C.; Thygesen, K. S. Energy level alignment and quantum conductance of functionalized metal-molecule junctions: Density functional theory versus GW calculations. *J. Chem. Phys.* **2013**, *139*, 184307.

(46) Hettler, M. H.; Schoeller, H.; Wenzel, W. Non-linear transport through a molecular nanojunction. *Eur. Phys. Lett.* **2002**, *57*, 571.

(47) Muralidharan, B.; Ghosh, A.; Datta, S. Conductance in Coulomb blockaded molecules - fingerprints of wave-particle duality. *Molec. Simulation* **2006**, *32*, 751–758.

(48) Muralidharan, B.; Ghosh, A. W.; Datta, S. Probing electronic excitations in molecular conduction. *Phys. Rev. B* **2006**, *73*, 155410.

(49) Hsu, L.-Y.; Tsai, T.-W.; Jin, B.-Y. Transport through a mixed-valence molecular transistor in the sequential-tunneling regime: Theoretical insight from the two-site Peierls–Hubbard model. *J. Chem. Phys.* **2010**, *133*, 144705.

(50) Refaely-Abramson, S.; Liu, Z.-F.; Bruneval, F.; Neaton, J. B. First-Principles Approach to the Conductance of Covalently Bound Molecular Junctions. *J. Phys. Chem. C* **2019**, *123*, 6379–6387.

(51) Goyer, F.; Ernzerhof, M.; Zhuang, M. Source and sink potentials for the description of open systems with a stationary current passing through. *J. Chem. Phys.* **2007**, *126*, 144104.

(52) Ernzerhof, M. A simple model of molecular electronic devices and its analytical solution. *J. Chem. Phys.* **2007**, *127*, 204709.

(53) Pickup, B. T.; Fowler, P. W. An analytic model for steady-state currents in conjugated systems. *Chem. Phys. Lett.* **2008**, *459*, 198–202.

(54) Stuyver, T.; Fias, S.; De Proft, F.; Geerlings, P. Back of the Envelope Selection Rule for Molecular Transmission: A Curly Arrow Approach. *J. Phys. Chem. C* **2015**, *119*, 26390–26400.

(55) Stuyver, T.; Blotwijk, N.; Fias, S.; Geerlings, P.; De Proft, F. Exploring Electrical Currents through Nanographenes: Visualization and Tuning of the through-Bond Transmission Paths. *Chem Phys Chem* **2017**, *18*, 3012–3022.

(56) Fias, S.; Stuyver, T. Extension of the source-sink potential approach to Hartree-Fock and density functional theory: A new tool to visualize the ballistic current through molecules. *J. Chem. Phys.* **2017**, *147*, 184102.

(57) Li, R.; Hou, S.; Zhang, J.; Qian, Z.; Shen, Z.; Zhao, X. Analysis of the contribution of molecular orbitals to the conductance of molecular electronic devices. *J. Chem. Phys.* **2006**, *125*, 194113.

(58) Solomon, G. C.; Gagliardi, A.; Pecchia, A.; Frauenheim, T.; Di Carlo, A.; Reimers, J. R.; Hush, N. S. The symmetry of single-molecule conduction. *J. Chem. Phys.* **2006**, *125*, 184702.

(59) Borges, A.; Solomon, G. C. An approach to develop chemical intuition for atomistic electron transport calculations using basis set rotations. *J. Chem. Phys.* **2016**, *144*, 194111.

(60) Solomon, G. C.; Andrews, D. Q.; Hansen, T.; Goldsmith, R. H.; Wasielewski, M. R.; Van Duyne, R. P.; Ratner, M. A. Understanding quantum interference in coherent molecular conduction. *J. Chem. Phys.* **2008**, *129*, 054701.

(61) Solomon, G. C.; Andrews, D. Q.; Goldsmith, R. H.; Hansen, T.; Wasielewski, M. R.; Van Duyne, R. P.; Ratner, M. A. Quantum Interference in Acyclic Systems: Conductance of Cross-Conjugated Molecules. *J. Am. Chem. Soc.* **2008**, *130*, 17301–17308.

(62) Fracasso, D.; Valkenier, H.; Hummelen, J. C.; Solomon, G. C.; Chiechi, R. C. Evidence for Quantum Interference in SAMs of Arylethynylene Thiolates in Tunneling Junctions with Eutectic Ga–In (EGaIn) Top-Contacts. *J. Am. Chem. Soc.* **2011**, *133*, 9556–9563.

(63) Ernzerhof, M.; Bahmann, H.; Goyer, F.; Zhuang, M.; Rochelau, P. Electron Transmission through Aromatic Molecules. *J. Chem. Theory Comput.* **2006**, *2*, 1291–1297.

(64) Solomon, G. C.; Herrmann, C.; Hansen, T.; Mujica, V.; Ratner, M. A. Exploring local currents in molecular junctions. *Nat. Chem.* **2010**, *2*, 223–228.

(65) Markussen, T.; Stadler, R.; Thygesen, K. S. The relation between structure and quantum interference in single molecule junctions. *Nano Lett.* **2010**, *10*, 4260–4265.

(66) Mayou, D.; Zhou, Y.; Ernzerhof, M. The zero-voltage conductance of nanographenes: simple rules and quantitative estimates. *J. Phys. Chem. C* **2013**, *117*, 7870–7884.

(67) Fowler, P. W.; Pickup, B. T.; Todorova, T. Z. Equiconducting molecular conductors. *Chem. Phys. Lett.* **2008**, *465*, 142–146.

(68) Fowler, P. W.; Pickup, B. T.; Todorova, T. Z.; Pisanski, T. Fragment analysis of single-molecule conduction. *J. Chem. Phys.* **2009**, *130*, 174708.

(69) Fowler, P. W.; Pickup, B. T.; Todorova, T. Z.; Myrvold, W. Conduction in graphenes. *J. Chem. Phys.* **2009**, *131*, 244110.

(70) Fowler, P. W.; Pickup, B. T.; Todorova, T. Z. A graph-theoretical model for ballistic conduction in single-molecule conductors. *Pure Appl. Chem.* **2011**, *83*, 1515–1529.

(71) Fowler, P. W.; Pickup, B. T.; Todorova, T. Z.; De Los Reyes, R.; Sciriha, I. Omni-conducting fullerenes. *Chem. Phys. Lett.* **2013**, *568–569*, 33–35.

(72) Fowler, P. W.; Pickup, B. T.; Todorova, T. Z.; Borg, M.; Sciriha, I. Omni-conducting and omni-insulating molecules. *J. Chem. Phys.* **2014**, *140*, 054115.

(73) Pickup, B. T.; Fowler, P. W.; Borg, M.; Sciriha, I. A new approach to the method of source-sink potentials for molecular conduction. *J. Chem. Phys.* **2015**, *143*, 194105.

(74) Pickup, B. T.; Fowler, P. W.; Sciriha, I. The Hückel SSP theory of the Pauli Spin Blockade of molecular electronic devices. *J. Chem. Phys.* **2016**, *145*, 204113.

(75) Fowler, W., P; Borg, M.; Pickup, B. T.; Sciriha, I. Molecular graphs and molecular conduction: the d-omni-conductors. *Phys. Chem. Chem. Phys.* **2020**, *22*, 1349–1358.

(76) Fowler, P. W.; Pickup, B. T.; Todorova, T. Z.; Myrvold, W. A selection rule for molecular conduction. *J. Chem. Phys.* **2009**, *131*, 044104.

(77) Goker, A.; Goyer, F.; Ernzerhof, M. Bond dissociation and correlation effects in molecular electronic devices. *J. Chem. Phys.* **2008**, *129*, 194901.

(78) Ono, K.; Austing, D.; Tokura, Y.; Tarucha, S. Current rectification by Pauli exclusion in a weakly coupled double quantum dot system. *Science* **2002**, *297*, 1313–1317.

(79) Kodera, T.; Ono, K.; Amaha, S.; Arakawa, Y.; Tarucha, S. Pauli spin blockade in a vertical double quantum dot holding two to five electrons. *J. Phys.: Conference Series* **2009**, *150*, 022043.

(80) Sylvester, J. J. On the relation between the minor determinants of linearly equivalent quadratic functions. *Philos. Mag.* **1851**, *1*, 295.

(81) Hubbard, J. Electron Correlations in Narrow Energy Bands. *Proc. Roy. Soc. A* **1963**, *276*, 238–257.

(82) Pariser, R.; Parr, R. G. A Semi-Empirical Theory of the Electronic Spectra and Electronic Structure of Complex Unsaturated Molecules. I. *J. Chem. Phys.* **1953**, *21*, 466–471.

(83) Pariser, R.; Parr, R. G. A Semi-Empirical Theory of the Electronic Spectra and Electronic Structure of Complex Unsaturated Molecules. II. *J. Chem. Phys.* **1953**, *21*, 767–776.

(84) Pople, J. Electron interaction in unsaturated hydrocarbons. *Trans. Faraday Soc.* **1953**, *49*, 1365.

(85) Zubarev, Z. N. Double-time Green's Functions in Statistical Physics. *Sov. Phys. Usp.* **1960**, *3*, 320.

(86) Csanak, G.; Taylor, H. S.; Yaris, R. Green's Function Technique in Atomic and Molecular Physics. *Advan. Atomic Molec. Phys.* **1971**, *7*, 287–361.

(87) Matsubara, T. A new approach to Quantum-Statistical Mechanics. *Prog. Theor. Phys.* **1955**, *14*, 351–378.

(88) Schirmer, J.; Cederbaum, L. S.; Walter, O. New approach to the one-particle Green's function for finite Fermi systems. *Phys. Rev. A* **1983**, *28*, 11237–1259.

(89) Barbieri, C.; Carbone, A. In *An Advanced Course in Computational Nuclear Physics: Bridging the Scales from Quarks to Neutron Stars*; Hjorth-Jensen, M., Lombardo, M. P., van Kolck, U., Eds.; Springer: Oxford, UK, 2017; Chapter Self-Consistent Green's Function Approaches, pp 571–644.

(90) Schirmer, J. *Many-Body Methods for Atoms, Molecules and Clusters*; Springer, 2018.

(91) Tamm, I. Relativistic interaction of elementary particles. *J. Phys.(USSR)* **1945**, *9*, 449.

(92) Dancoff, S. M. Non-adiabatic meson theory of nuclear forces. *Phys. Rev.* **1950**, *78*, 382.

(93) Rocheleau, P.; Ernzerhof, M. Molecular conductance obtained in terms of orbital densities and response functions. *J. Chem. Phys.* **2009**, *130*, 184704.

(94) Zhou, Y. X.; Ernzerhof, M. Equiconducting molecular electronic devices. *J. Chem. Phys.* **2010**, *132*, 104706.

(95) Ernzerhof, M.; Goyer, F. Conjugated molecules described by a one-dimensional Dirac equation. *J. Chem. Theory Comput.* **2010**, *6*, 1818–1824.

(96) Goyer, F.; Ernzerhof, M. Correlation effects in molecular conductors. *J. Chem. Phys.* **2011**, *134*, 174101.

(97) Ernzerhof, M. Simple orbital theory for the molecular electrician. *J. Chem. Phys.* **2011**, *135*, 014104.

(98) Rocheleau, P.; Ernzerhof, M. Extension of the source-sink potential (SSP) approach to multichannel quantum transport. *J. Chem. Phys.* **2012**, *137*, 174112.

(99) Ernzerhof, M. Coherent molecular transistor: control through variation of the gate wave function. *J. Chem. Phys.* **2014**, *140*, 114708.

(100) Ernzerhof, M.; Bélanger, M.-A.; Mayou, D.; Aram, T. N. Simple

model of a coherent molecular photocell. *J. Chem. Phys.* **2016**, *144*, 134102.

(101) Sols, F.; Macucci, M.; Ravaioli, U.; Hess, K. Theory for a quantum modulated transistor. *J. Appl. Phys.* **1989**, *66*, 3892–3906.

(102) Fisk, S. Polynomials, roots, and interlacing. 2006; arXiv: math/0612833v2 [math.CA].

(103) Maplesoft, *Maple 2018*; Maplesoft: Waterloo Maple Inc., Waterloo, Ontario, 2018.

(104) Pickup, B. T.; Goscinski, O. Direct calculation of ionization energies. I. Closed shells. *Mol. Phys.* **1973**, *26*, 1013–1035.

(105) Baker, J.; Pickup, B. T. A method for molecular ionization potentials. *Chem. Phys. Lett.* **1980**, *76*, 537–541.

(106) Baker, J.; Pickup, B. T. Propagator calculations of molecular ionization potentials. *Mol. Phys.* **1983**, *49*, 651–662.

(107) Corzo, H. H.; Galano, A.; Dolgounitcheva, O.; Zakrzewski, V. G.; Ortiz, J. V. NR2 and P3+: Accurate, Efficient Electron-Propagator Methods for Calculating Valence, Vertical Ionization Energies of Closed-Shell Molecules. *J. Phys. Chem. A* **2015**, *119*, 8813–8821.

(108) Coulson, C. A.; Rushbrooke, G. S. Note on the method of molecular orbitals. *Proc. Camb. Phil. Soc.* **1940**, *36*, 193–200.

(109) Landau, L. D.; Lifschitz, E. M. *Quantum Mechanics, Non-relativistic Theory (Volume 3 of A Course in Theoretical Physics)*, 3rd ed.; Pergamon Press, Oxford, UK, 1977; pp 55–57.

(110) Knight, J. W.; Wang, X.; Gallandi, L.; Dolgounitcheva, O.; Ren, X.; Ortiz, J. V.; Rinke, P.; Körzdörfer, T.; Marom, N. Accurate Ionization Potentials and Electron Affinities of Acceptor Molecules III: A Benchmark of GW Methods. *J. Chem. Theory Comput.* **2016**, *12*, 615–626.